Calhoun: The NPS Institutional Archive

DSpace Repository

Theses and Dissertations | 1. Thesis and Dissertation Collection, all items

1987

Effects of 67.5 MeV electron irradiation on Y-Ba-Cu-O high-temperature superconductors.

Sweigard, Eric Lynn; Buskirk, Fred R.

https://hdl.handle.net/10945/22250

Downloaded from NPS Archive: Calhoun

http://www.nps.edu/library

Calhoun is the Naval Postgraduate School's public access digital repository for research materials and institutional publications created by the NPS community. Calhoun is named for Professor of Mathematics Guy K. Calhoun, NPS's first appointed -- and published -- scholarly author.

Dudley Knox Library / Naval Postgraduate School
411 Dyer Road / 1 University Circle
Monterey, California USA 93943

NAVAL POSTGRADUATE SCHOOL
Monterey, California

THESIS

S93522

EFFECTS OF 67.5 MeV ELECTRON IRRADIATION ON Y-Ba-Cu-OAND Gd-Ba-Cu-O HIGH-TEMPERATURE SUPERCONDUCTORS

by

Eric Lynn Sweigard

December 1987

Thesis Advisor: F. R. Buskirk

Approved for public release; distribution is unlimited.

T239282

REPORT DOCUMENTATION PAGE

1a REPORT SECURITY CLASSIFICATION UNCLASSIFIED	1b RESTRICTIVE MARKINGS
2a SECURITY CLASSIFICATION AUTHORITY	3 DISTRIBUTION / AVAILABILITY OF REPORT Approved for public release; Distribution is unlimited
2b DECLASSIFICATION / DOWNGRADING SCHEDULE	
4 PERFORMING ORGANIZATION REPORT NUMBER(S)	5 MONITORING ORGANIZATION REPORT NUMBER(S)
6a NAME OF PERFORMING ORGANIZATION NAVAL POSTGRADUATE SCHOOL 6b OFFICE SYMBOL (If applicable) CODE 61	7a NAME OF MONITORING ORGANIZATION NAVAL POSTGRADUATE SCHOOL
6c ADDRESS (City, State, and ZIP Code) Monterey, California 93943-5000	7b ADDRESS (City, State, and ZIP Code) Monterey, California 93943-5000
8a NAME OF FUNDING / SPONSORING ORGANIZATION 8b OFFICE SYMBOL (If applicable)	9 PROCUREMENT INSTRUMENT IDENTIFICATION NUMBER
8c ADDRESS (City, State, and ZIP Code)	10 SOURCE OF FUNDING NUMBERS PROGRAM ELEMENT NO / PROJECT NO / TASK NO / WORK UNIT ACCESSION NO

11 TITLE (Include Security Classification)
Effects of 67.5 MeV Electron Irradiation on Y-Ba-Cu-O and Gd-Ba-Cu-O High-Temperature Superconductors (Unclassified)

12 PERSONAL AUTHOR(S)
Sweigard, Eric L.

13a TYPE OF REPORT	13b TIME COVERED	14 DATE OF REPORT (Year, Month, Day)	15 PAGE COUNT
Master's Thesis	FROM _____ TO _____	1987, December	84

16 SUPPLEMENTARY NOTATION

17 COSATI CODES			18 SUBJECT TERMS (Continue on reverse if necessary and identify by block number)
FIELD	GROUP	SUB-GROUP	High-Temperature Superconductors; Radiation Effects; Electron Irradiation; Superconductivity

19 ABSTRACT (Continue on reverse if necessary and identify by block number)

High-temperature superconductors ($YBa_2Cu_3O_{6+\delta}$ and $GdBa_2Cu_3O_{6+\delta}$, both with $\delta \leq 1$) with $T_c \approx 92K$ and manufactured at the University of Houston were irradiated with 67.5 MeV electrons at fluences of 10^{13}, 10^{14}, 10^{15} and 5×10^{15} electrons/cm^2. The irradiation effects were studied by analyzing resistance versus temperature curves developed using the four-probe resistance measuring technique. The YBaCuO sampleshowed irradiation effects in the form of a normal state resistance drop after the 10^{13} irradiation (.3 Mrad) and an isolated failure to achieve total superconductivity above 77K after the 10^{14} irradiation (3 Mrad). The same sample re-established its high-T_c (92K) after subsequent irradiations. This was presumed to indicate microscopic damage to superconducting channels. It also displayed granular crumbling in the vicinity of the electrical contacts. This was interpreted as an effect of the differences in thermal expansion rates between the contacts and the superconductor.

20 DISTRIBUTION / AVAILABILITY OF ABSTRACT	21 ABSTRACT SECURITY CLASSIFICATION
☒ UNCLASSIFIED/UNLIMITED ☐ SAME AS RPT ☐ DTIC USERS	Unclassified
22a NAME OF RESPONSIBLE INDIVIDUAL Prof. Fred R. Buskirk	22b TELEPHONE (Include Area Code) (408) 646-2765 22c OFFICE SYMBOL Code 61Bs

DD FORM 1473, 84 MAR 83 APR edition may be used until exhausted
All other editions are obsolete

SECURITY CLASSIFICATION OF THIS PAGE

☆ U.S. Government Printing Office 1986—606-24-

BLOCK 19. (Continued) The GdBaCuO sample showed no such effect until its 10^{15} irradiation where it showed localized crubling as well. In view of these results the GdBaCuO was concluded to be superior to YBaCuO for use in high radiation environments, although neither material should require any extraordinary shielding in such environments. Difficulties maintaining electrical contacts on the superconductors for these measurements hindered the conclusiveness of the data.

Approved for public release; distribution is unlimited.

Effects of 67.5 MeV Electron Irradiation on Y-Ba-Cu-O and Gd-Ba-Cu-O High-Temperature Superconductors

by

Eric Lynn Sweigard
Lieutenant, United States Navy
B.S., United States Naval academy, 1979

Submitted in partial fulfillment of the
requirements for the degree of

MASTER OF SCIENCE IN PHYSICS

from the

NAVAL POSTGRADUATE SCHOOL
December 1987

ABSTRACT

High-temperature superconductors ($YBa_2Cu_3O_{6+\delta}$ and $GdBa_2Cu_3O_{6+\delta}$, both with $\delta \leq 1$) with $T_c \approx 92$ K and manufactured at the University of Houston were irradiated with 67.5 MeV electrons at fluences of 10^{13}, 10^{14}, 10^{15}, and 5×10^{15} electrons/cm^2. The irradiation effects were studied by analyzing resistance versus temperature curves developed using the four-probe resistance measuring technique. The $YBa_2Cu_3O_{6+\delta}$ sample showed irradiation effects in the form of a normal state resistance drop after the 10^{13} irradiation (.3 Mrad) and an isolated failure to achieve total superconductivity above 77 K after the 10^{14} irradiation (3 Mrad). The same sample re-established its high-T_c (92 K) after subsequent irradiations. This was presumed to indicate microscopic damage to superconducting channels. It also displayed granular crumbling in the vicinity of the electrical contacts. This was interpreted as an effect of the differences in thermal expansion rates between the contacts and the superconductor. The $GdBa_2Cu_3O_{6+\delta}$ sample showed no such effects until its 10^{15} irradiation where it showed localized crumbling as well. In view of these results, the $GdBa_2Cu_3O_{6+\delta}$ was concluded to be superior to $YBa_2Cu_3O_{6+\delta}$ for use in high irradiation environments, although neither material should require any extraordinary shielding in such environments. Difficulties maintaining electrical contacts on the superconductors for these measurements hindered the conclusiveness of the data.

SCHOOL
93943-5002

TABLE OF CONTENTS

I. INTRODUCTION 8

A. PURPOSE OF EXPERIMENT 8

1. Statement of Experiment 8

2. Overview 8

3. Potential Applications of Superconductors 9

B. HISTORY 11

C. PREVIOUS RESEARCH 12

II. THEORY 14

A. SUPERCONDUCTOR THEORY (GENERAL) 14

B. SUPERCONDUCTOR THEORY (RECENT DEVELOPMENTS) 27

C. RADIATION THEORY 36

III. EXPERIMENTAL PROCEDURES 42

A. RADIATION FACILITY 42

B. RESISTANCE MEASURING FACILITY 48

IV. EXPERIMENTAL RESULTS 52

V. CONCLUSIONS AND RECOMMENDATIONS FOR FUTURE WORK 74

A. CONCLUSIONS 74

B. RECOMMENDATIONS FOR FUTURE WORK 77

LIST OF REFERENCES 80

INITIAL DISTRIBUTION LIST 82

ACKNOWLEDGMENTS

My most sincere thanks to C. W. Huang, F. A. Junga, and L. J. Dries of the Research and Development Division of Lockheed Missiles and Space Co., Inc. , for providing the samples, the measurement facilities, and an advance copy of their paper. Thanks especially to Larry, for the answers to my seemingly endless, and often unenlightened, questions. I thoroughly enjoyed going to Lockheed and working with him.

Thanks also to J. C. Ritter and G. P. Summers of the Naval Research Laboratory in Washington, D. C., for providing an advance copy of their paper and for answering several key questions.

Special thanks to Professors F.R. Buskirk and X.K. Maruyama, first of all, for offering me this topic; secondly, for guiding me through it; and, finally, for making my memory of the whole thesis experience a positive one.

Finally, countless thanks to Don Snyder. I have found, in the two and a half years I've known him, that, for him, the word "impossible" held absolutely no meaning. I am very grateful for all his help with this experiment as well as for everything else with which he helped since I first moved into the LINAC.

I. INTRODUCTION

A. PURPOSE OF EXPERIMENT

1. Statement of Experiment

Two high-temperature (T_C~92K) $YBa_2Cu_3O_{6+\delta}$ and $GdBa_2Cu_3O_{6+\delta}$ ($\delta \leq 1$ for both) superconducting samples manufactured by C. W. Chu (University of Houston) were irradiated with 67.5 MeV electrons at fluences ranging from 10^{13} to $5x10^{15}$ electrons/cm^2 in order to study the effects that high-radiation environments might have on these materials. The results were plotted on resistance versus temperature plots and compared with results of the Naval Research Laboratory (NRL) experiment with 56 MeV electrons [Ref. 1] and the Lockheed Missiles and Space Company experiment with 1.17 and 1.33 MeV gamma rays [Ref. 2].

2. Overview

Since the development of the wheel, inventors, engineers and scientists have searched for ways to reduce system energy losses and minimize frictional effects; to find a perpetual motion machine of sorts. While the laws of thermodynamics prohibit perpetual motion, it seems that the phenomenon of superconductivity may provide the avenue of closest approach to such a system.

Superconductors, with their unusual electromagnetic properties, have already been used in ultra-high field magnets, nearly-frictionless bearings and nearly-lossless transmission wires, to name a

few applications. One of the factors complicating the practical applications of superconductivity has been the very low temperatures at which they must be maintained in order to superconduct. Until recently, all superconductors required liquid helium to cool the materials to their superconducting temperatures. As liquid helium is both expensive to make and difficult to handle, the systems requiring superconducting components were usually quite expensive to build and operate. Very recent (1987) developments in the superconductivity field have led to compounds which superconduct at temperatures accessible with liquid nitrogen as the cooling medium. Since liquid nitrogen is much less expensive to make and easier to handle, an incredible surge of scientific and industrial attention has come to the field of superconductivity.

3. Potential Applications of Superconductors

The impact that these new developments have made on the considerations of potential applications was evidenced in the congressional debate regarding delaying the proposed $4.4 billion superconducting super collider (SSC) project until such time as the high field magnets could be made with the new compounds instead of the previously planned lower temperature superconductors. With the Strategic Defense Initiative's (SDI's) focus on space, these virtually lossless electrical conductors become particularly attractive for space applications as well. Prior to the recent high temperature developments, the Federal Government spent an annual average of $15 million for superconductivity research and development, a third of which was provided

by the U.S. Navy [Ref. 3]. Some of the Navy's proposed research topics include:

a. High energy particle shields: Comprised of large-field, lightweight superconductive magnets, these shields might deflect charged particles in ABM or ASAT particle beams.

b. Energy storage/batteries: Superconducting coils or magnets permit compact and highly efficient energy densities far surpassing chemical energy storage systems. These systems could be charged by solar radiation in space.

c. Gyrotrons/FEL's: Free electron lasers, gyrotrons, and other particle accelerators utilize magnets which could be replaced by superconducting magnets at higher field strengths for less input power.

d. Communications satellites: Superconductors permit reductions in satellite size, reduction in weight and power consumption and afford greater bandwidths than traditional systems.

e. Battle management/information processing: High speed superconductive data processors permit managing large volumes of tactical and strategic data in real time. Extremely important for expected scenarios in which SDI would operate.

f. Rail guns/E-M launchers: Superconducting magnets can provide field intensities to accelerate KEW (kinetic energy weapon) projectiles to potential speeds of ~62 miles/second with estimated potential firing rates of 60 shots/second [Ref. 4]. Same application on Earth's surface may permit electromagnetic launch of missiles to reduce booster size and signatures.

As all of these applications place the new compounds in potentially high radiation environments, research must be done in order to determine whether these materials can withstand such environments without degradation. This experiment, therefore, investigates one aspect (electron irradiation effects) of the extreme conditions which these environments might offer.

B. HISTORY

Superconductivity was first observed in 1911 at Leiden by Kammerlingh Onnes, who three years earlier had pioneered the liquification of helium. Using the fruits of his labor, he was able to cool substances to temperatures below 4.2 K, a previously inaccessible temperature. While investigating the relationship between the temperature and electrical resistance of mercury, he observed that the electrical resistance completely vanished at a "critical temperature" (T_c) of 4.15 K. Surmising that the mercury had undergone a state change, Onnes labeled the new-found state the "superconducting state." [Ref. 5]

Since Onnes' discovery, a plethora of other superconducting materials (including elements, alloys, and intermetallic compounds) were found to have critical temperatures ranging from just above absolute zero (eg: 0.023 K for CRb_x) [Ref. 6] to about 20 K (e.g., 23.2 K for Nb_3Ge) [Ref. 6]. While several of these superconductors have been used in various applications, their low critical temperatures still required the use of liquid helium to enter the superconducting state. In early 1986, two researchers at IBM's Swiss laboratory, J. Georg Bednorz and K. Alex Mueller, pursued their rather paradoxical idea that the same microscopic properties which made ceramic materials such good electrical insulators in their normal states might possibly contribute to meeting the requirements for entering the superconducting state. Indeed, their suspicions proved correct. In September 1986, the pair reported observing critical temperatures of

approximately 34 K in the compound $Ba_xLa_{5-x}Cu_5O_{5(3-y)}$ where x=1 and 0.75 and y>0 [Ref. 8]. The pair recently won the 1987 Nobel Prize for Physics for this work.

Following the lead of Bednorz and Mueller, physicists around the world began the hunt for higher temperature superconductors. On 29 January 1987, C. W. Chu, of the University of Houston, broke the elusive liquid nitrogen barrier when he observed evidence of superconductivity in a rare earth ceramic compound of $YBa_2Cu_3O_{7-x}$ (x<1) at a landmark temperature of 93 K [Ref 9]. With this discovery came an incredible upsurge of interest in superconductor technology. With the present materials capable of superconductivity above liquid nitrogen temperatures, applications once ignored as too expensive or difficult to operate (due to the liquid helium requirements) became the most highly focused upon field of research to arise in many years.

C. PREVIOUS RESEARCH

As the discovery of the $LBa_2Cu_3O_{6+\delta}$ (where L=Y or all rare earths except Ce and Pr and $0< \delta <1$) compounds is so recent, there is very little available literature regarding existing irradiation effects research. This experiment is a follow-on to research conducted by C. Y. Huang et al at Lockheed Missiles and Space Company (Palo Alto, California) regarding Co^{60} gamma (E_γ = 1.17, 1.33 MeV) irradiation effects on $YBa_2Cu_3O_{6+\delta}$ samples manufactured by C. W. Chu et al. at University of Houston. Their results are discussed in this paper and published in Reference 2.

Near the completion of this paper, W. G. Maisch et al. from Naval Research Laboratory (NRL) reported results from an experiment of almost identical conditions as this experiment. Their results are published in Reference 1.

II. THEORY

A. SUPERCONDUCTOR THEORY (GENERAL)

Superconductivity is a molecular state wherein a substance loses all (measureable) resistance to electrical flow. Superconductors, as we presently know them, exist naturally in the "normal state." That is, in their normal state the superconductors exhibit a finite electrical conductivity. In order to make the transition to the superconducting state, a superconductor must be cooled to its "transition" or "critical" temperature. When the substance reaches that temperature, there is a dramatic disappearance of electrical resistance. It was this feature, the sudden drop in resistance, which convinced Onnes to label this phenomenon as a change of state. [Ref. 5]

Scientists typically employ two major tests in determining whether a substance is superconducting or not. The first method, known as the "four probe method" is susceptible to considerably more false alarms than the second and is, therefore, not always as conclusive unless the indications can be reliably reproduced. It does, however, provide more information about the before and after conditions leading up to the state change than the second method. The second method is more of a go-no-go gauge than a measurement. It exploits a phenomenon known as the Meissner effect to determine whether or not superconductivity has occurred. If the Meissner effect is observed, we conclude that the substance must be in the superconducting state.

The four-probe method (Figure 1) determines the electrical resistance present in a substance by measuring the voltage induced across the sample when a given current is applied through the sample. The method derives its name from the four points on the sample upon which the two voltage and two current leads are affixed. All substances have a bulk property known as resistivity, ρ, which is non zero in the normal state. The inverse of this property is the electrical conductivity, $\sigma = 1/\rho$. If we consider a conducting channel of cross-sectional area, A, and length, l, we can express the resistivity in terms of current, I, and voltage, V:

$$\rho = \frac{V/l}{I/A} \qquad (1)$$

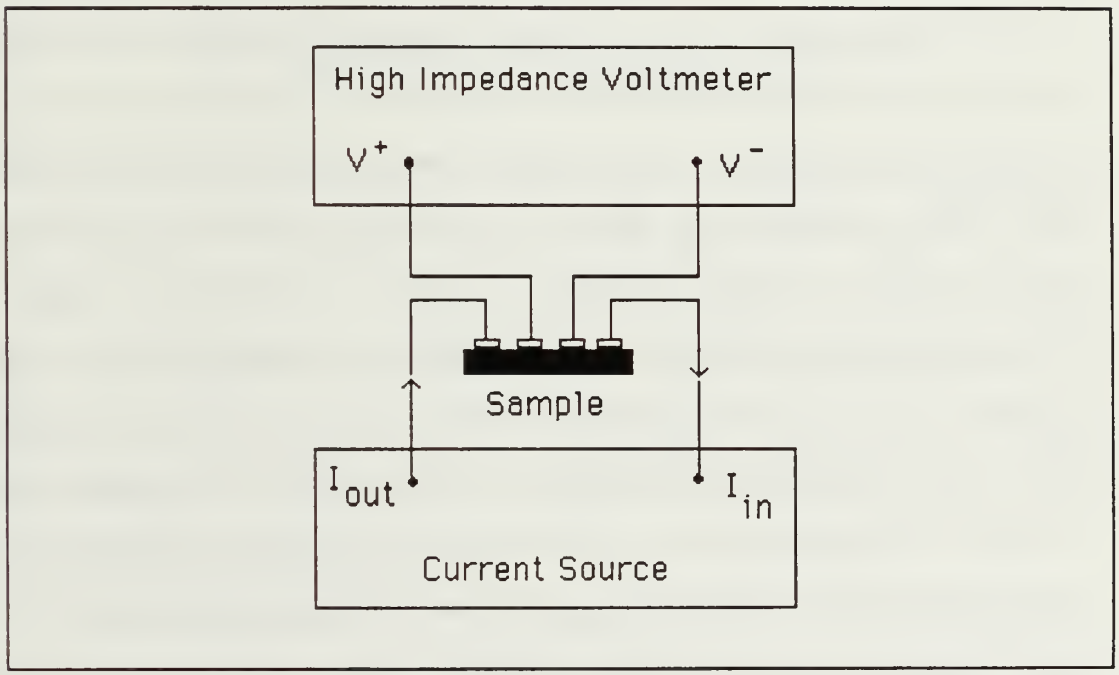

Figure 1

The Four-Probe Method for Measuring Conductivity of a Substance

In testing for superconductivity, we are generally unconcerned with the exact resistivity of the substance in the normal state; however, so long as the measurement leads maintain the same contact points for successive measurements, the normal state resistivities can be compared for signs of variation due to some laboratory-induced condition (e.g., radiation exposure). It is easy to see that, if the voltage goes to zero, the resistivity goes to zero and superconductivity can be assumed (unless an electical connection opens).

The second method, exploiting the Meissner effect, requires no electrical inputs and no measurements other than that of temperature. The Meissner effect was first discovered in 1933 by W. Meissner and R. Ochsenfeld when they showed that a superconductor immersed in a longitudinal magnetic field, then cooled to its critical temperature, would expel the lines of induction (Figure 2). Similarly, if the superconductor was cooled to its critical temperature in a zero magnetic field, then exposed to a non-zero field while still in the superconducting state, it would exclude the lines of induction. These two phenomena, the expulsion and exclusion of magnetic flux from the interior of the superconductor, collectively represent the Meissner effect. The most dramatic method of observing the Meissner effect is to place a permanent (e.g., cobalt samarium) magnet above a superconductor sample and immerse the pair in liquid helium (or, with the new materials, liquid nitrogen suffices). As the superconductor passes its critical temperature, it enters the superconducting state and it

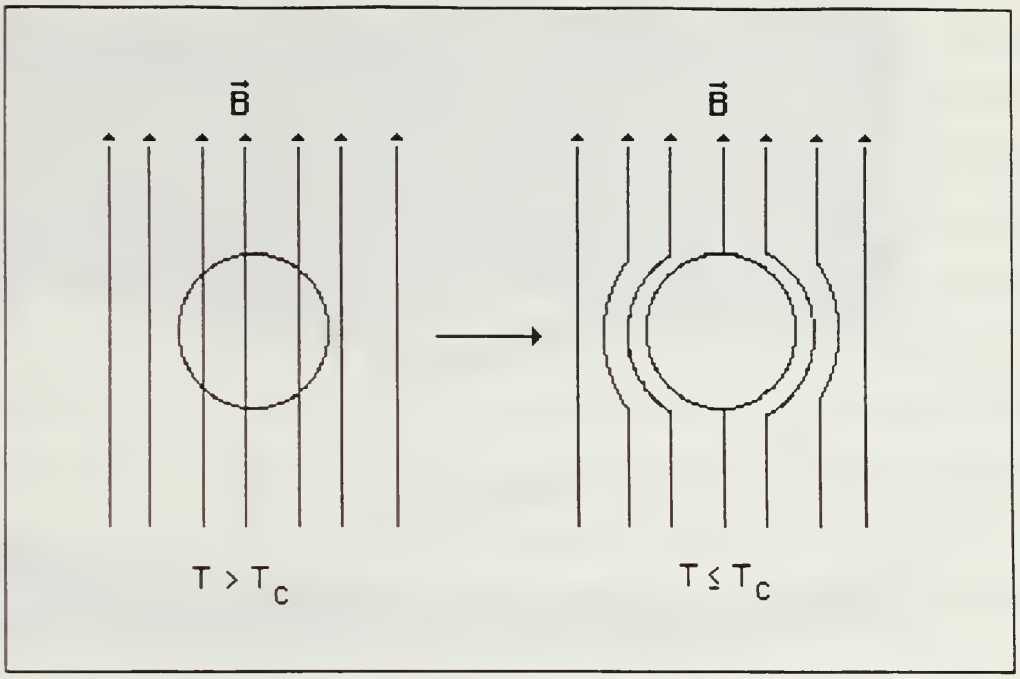

Figure 2

Meissner Effect: Magnetic Flux Expulsion in a Superconducting Sphere

expels the magnetic flux. The lines of flux, having been expelled from the interior of the sample, form a force field-like cushion which is unable to penetrate the sample, thus causing the magnet to levitate above the superconductor (Figure 3). Once the temperature of the sample is raised above its critical temperature, the magnetic flux again penetrates the sample and the magnet falls gravitationally to the superconductor beneath it.

Another consequence of the Meissner effect arises in the form of persisting currents. According to Lenz's law, an induced current always flows in such a direction as to oppose the magnetic flux change

Figure 3

The Meissner Effect as Represented by Magnetic Levitation
[Ref. 10:p. 486].

which produced it. When a superconducting ring is placed in a magnetic field, the free electrons flow, unimpeded, such that they oppose the magnetic flux lines. In this sense, the superconductor acts as a perfect diamagnet [Ref. 10]. Once the free electrons begin to flow in the ring, having no electrical resistance, they continue to flow—even after the magnetic field is removed. In 1924, Onnes was able to observe such a persistent current in superconducting lead (Pb) coils for a period of twelve hours without any detectable decay of current. Using the formula for current decay in an R-L circuit:

$$I(t) = i_0 \exp\left(\frac{-Rt}{L}\right) \qquad (2)$$

where R is the resistance and L the self-inductance of a material, Onnes calculated the resistance of his lead coil to be less than 10^{-15} R_0', where R_0' is the residual resistance for a material extrapolated as if it never entered the superconducting state [Ref. 11]. In 1956 at MIT, S. C. Collins completed an experiment wherein he had maintained a superconducting ring below its critical temperature for the previous two and a half years. During this time, he observed no perceptible decay in current. Based on the precision of his equipment, he estimated the resistivity to be approximately 10^{-21} ohm-cm. This is approximately twelve orders of magnitude less than the resistivity of the purest copper at low temperatures. [Ref. 12]

While immersion in a magnetic field can induce persistent currents in a superconductor, there are limits to the field strengths under which a superconductor can remain superconducting. This limit is referred to as the critical field, H_c , and it is dependent upon the existing temperature of the particular superconducting material. The term, critical temperature, typically refers to the temperature at which a material transits to the superconducting state under zero (discounting the earth's field) external field. In actuality, there is a different critical temperature for each applied magnetic field until the field is so strong that the material cannot superconduct even at absolute zero. Figure 4 shows this relationship for a generic superconductor. Equation (3), derived experimentally by Keesom in 1935, approximates this relationship for previously known materials:

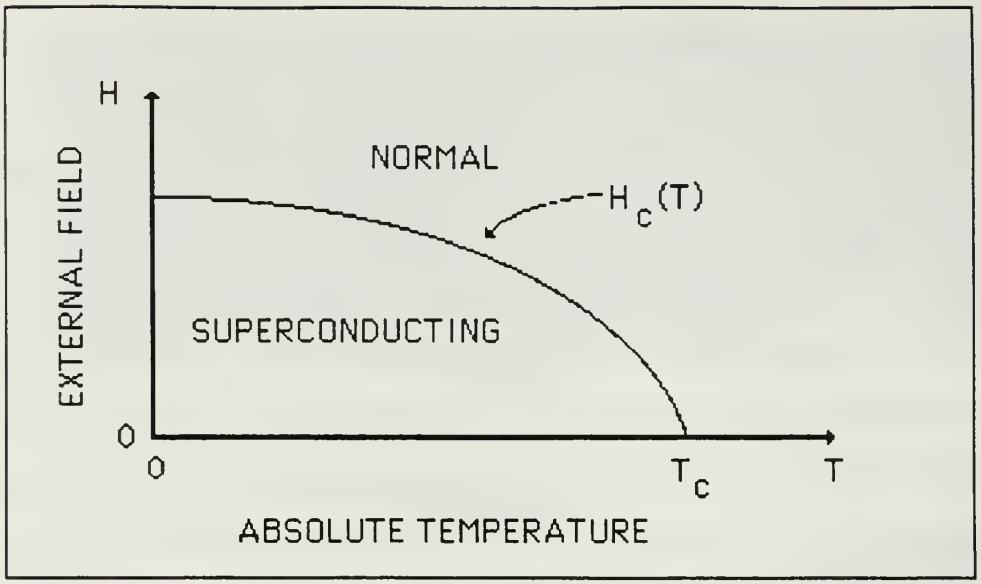

Figure 4

Phase Diagram of a Superconductor in the H-T Plane [Ref. 13]

$$H_c \approx H_0 \left[1 - \left(\frac{T}{T_c} \right)^2 \right] \tag{3}$$

where H_0 is the critical field at absolute zero [Ref. 12]. An associated characteristic of superconductors, known as the critical current, actually predated the discovery of critical fields. In 1913, Onnes found that after a certain amount of current, the critical current, was passed through a superconducting wire, superconductivity ceased [Ref. 5]. In 1915, Silsbee showed that the critical current was merely that current which produced a magnetic field of sufficient strength to quench superconductivity. He arrived at equation (4) for the critical field in terms of current in a long round wire:

$$H_c = \frac{2I}{r} \tag{4}$$

where r is the wire's radius. This was thought to be the major limiting factor in the development of strong superconducting magnets, however, it was later found that, while Silsbee's hypothesis held for pure unstrained metallic elements, it did not hold for alloys and compounds. [Ref. 11]

In 1950, Maxwell showed that lattice vibrations might contribute to superconductivity when he found that the critical temperatures of some mercury isotopes varied as the inverse of the square root of the isotopic mass, or:

$$M^{1/2} T_c = \text{constant} \tag{5}$$

for a given series of isotopes [Ref. 10]. In 1950, no complete microscopic theory of superconductivity existed. It was the isotope effect that provided the impetus to pursue a theory based on phonon-electron interactions, which eventually led to the widely accepted BCS theory of superconductivity.

In 1957, Bardeen, Cooper, and Schrieffer published a paper entitled "The Theory of Superconductivity." In their introductory remarks they summarized the problems which had for so long eluded a comprehensive microscopic description of superconductivity:

> The main facts which a theory ... must explain are (1) a second-order phase transition at the critical temperature, (2) an electronic specific heat varying as $\exp(-T_0/T)$ near $T=0$ ... (3) the Meissner effect ($\mathbf{B}=0$), (4) effects associated with infinite conductivity ($\mathbf{E}=0$), and (5) the dependence of T_c on isotopic mass ..." [Ref. 14]

The trio went on to propose a theory which explained all the above. The BCS theory, as it is now known, won them the Nobel prize in 1972.

The BCS theory is based upon the interaction of the free electrons with their surrounding lattice ions. Since the theory explains a microscopic quantum state, it cannot accurately be described in a classical sense. Classical descriptions can only serve to aid in providing a conceptualization of superconductivity. This conceptual approach can be quite confusing in itself because certain quantum mechanical phenomena do not "make sense" classically. There are a few instances in BCS theory where the conceptual description drops into that pitfall.

The BCS theory emphasizes an electron-phonon-electron interaction which results in a pairing of electrons in a solid. These electron pairs are formed when a free electron in a solid passes between lattice ions. The Coulomb attraction between the different charges causes the ions to move towards the electron, thus slightly distorting the lattice structure. Once the lattice forces overcome the departing electron's Coulomb attraction, the ions are elastically snapped back from their outstretched locations, oscillating about their equilibrium lattice positions. These oscillations propagate through the lattice at the speed of sound in the form of a moving region of higher positive charge density. The propagator is a phonon which was, in effect, "emitted" by the passing electron. This phonon, carrying momentum

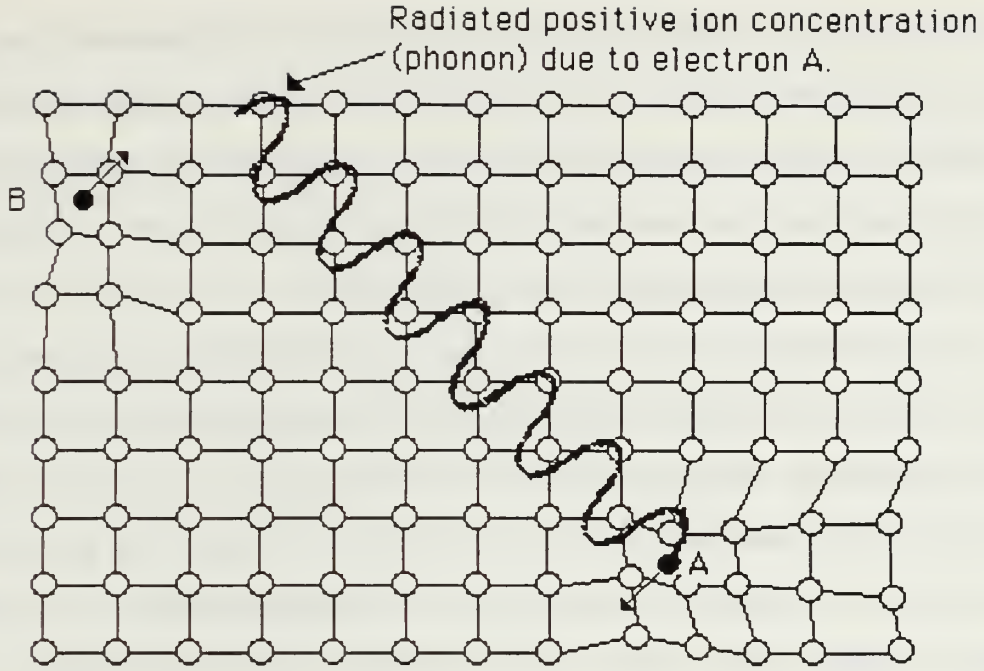

Figure 5

Conceptual Representation of a Lattice Being Traversed By a Pair of Electrons (Cooper Pair), Each Emitting Phonons and Being Influenced by Them
[Ref. 5:p. 10]

from its parent electron, can now Coulomb interact and give up its momentum to another electron. The first electron has essentially interacted with the second by exchanging momentum through a Coulomb attraction, using the phonon as an intermediary. The BCS theory explains that two electrons can pair when the attractive force is sufficiently strong to overcome their Coulomb repulsion. If the thermal energy of the material is too high (greater than T_c) then the lattice will be subjected to too much random thermal motion and the attractive force will be too insignificant to effect pairing. At

sufficiently low temperatures (T_c and below) this random motion will be reduced such that the attractive force is able to hold the electrons together. Under such conditions, the electrons form pairs known as Cooper pairs and, according to BCS theory, they are the mechanism by which superconductivity occurs. [Ref. 10]

Cooper pairs are loosely bound and, therefore, relatively large. Since they are loosely bound, they are also rather unstable. The average maximum distance over which these pairs can be formed is termed the coherence length and it is typically on the order of micrometers. Within a single coherence length there are, therefore, great numbers of other electrons which should participate in the phonon interactions. Although the individual pairs are unstable, if the conditions are such that the many other electrons within the coherence length can also pair, then the system as a whole will be quite stable. In other words, if there exists a high probability of pairing, then every broken pair should immediately form a new pair thus rendering the system, at any instant, predominantly paired. [Ref. 10]

The electron-phonon-electron interaction involves the conservation of momentum for the Cooper pair, and therefore dictates that the total momentum of any given pair is constant. If all the pairs in the system have the same total momentum, then the breaking up of pairs will result in almost instantaneous recombination with other broken pairs. This is because the broken pairs, having had the same total momentum, will be able to easily exchange a phonon. The final result is that the maximum number of Cooper pairs will be present. The

system accomplishes this by requiring the total momentum of each pair to be equal to zero. BCS theory reaches this conclusion by quantum mechanical calculations which show that when the pairs have the same total momentum, the pair-formation wave functions are in phase, adding constructively, thus resulting in a high total probability for pair formation throughout the system. With no electric field, quantum mechanical symmetry considerations require that the total momentum must be zero for all pairs [Ref. 10]. Classically, this is confusing because it implies that each electron in the pair must be moving with equal and opposite momenta while maintaining their interaction. Quantum mechanically, however, the electron wave functions (being equal and opposite) can continue to interact over large distances [Ref. 15]. While this pairing has been described for only one system (i.e., over one coherence length), it applies throughout the entire lattice because the size of the Cooper pairs provides sufficient spatial conditions for multiple system overlap [Ref. 10].

The key to superconductivity lies in the zero total momentum of each Cooper pair. When an electric field is applied to the superconductor, the Cooper pairs move under its influence such that all their centers of mass move together with the same momenta. They do so without any of the resistance encountered in the normal state. This is not because thermally induced random lattice vibrations and structural imperfections do not exist (even though the former are reduced at lower temperatures), but it is due to the way in which the Cooper pairs react to scattering. Since each electron in a pair is identical

except in their exactly opposite momenta, the scattering of one electron effects the other member of the pair in exactly the opposite way, thus preserving the pair's total momentum. In other words, the lattice cannot alter the flow of current so long as the Cooper pairs exist. [Ref. 15]

Superconductors have been classified into two types based upon their reaction to magnetic fields. Type I superconductors completely exclude magnetic flux until the field strength exceeds H_c and the material enters the normal state. They carry the current in a very thin ($\sim 10^{-5}$ cm thick) surface layer and, although they can carry very large current densities ($\sim 10^{8}$ A-cm^{-2}), their resulting surface currents are typically only about 1000 A-cm^{-1} [Ref. 5]. Type I superconductors also have relatively low critical fields up to approximately 800 A-cm^{-1} [Ref. 16]. They are, therefore, poorly suited to magnetic applications. This was originally quite discouraging because the concept of zero electrical resistance meant that electromagnets could be produced with much less energy input (than with conventional magnets) to obtain the same fields. The low Hc values of the type I materials severely limited these applications.

The type II superconductors have a more complicated reaction to magnetic fields. Typically alloys, the type II materials are similar to the type I materials up to a penetration critical field, H_{c1}. At higher magnetic fields, the type II superconductors permit the flux to partially penetrate the sample up to a cessation critical field of H_{c2}, where the magnetic flux completely penetrates the sample and elevates it to

the normal state [Ref. 15]. This is made possible by the size of the type II Cooper pairs. The pairs are small enough that the flux lines are able to pass through the sample along localized filaments causing those channels to lose their superconductivity. The material is said to be in a mixed state—partially superconducting and partially normal. The adjacent filaments remain in the superconducting state, however, and the material is therefore able to withstand much higher fields [Ref. 10]. These materials are quite well suited for the magnetic applications and have been shown to withstand field strengths of up to 150 kgauss (15 Tesla) while still carrying bulk current densities near 10^6 A/cm^2 [Ref. 5, p.1]. Type I superconductors are typically the pure elements such as mercury, tin, lead, and niobium. Near absolute zero, mercury has a critical field (B_c) of only 0.041 T. The type II superconductors are typically compounds. An example of the type II superconductors is Nb_3Sn with an onset critical field (B_{c1}) of 0.019 T and a cessation critical field (B_{c2}) of 22 T. [Ref. 15]

B. SUPERCONDUCTOR THEORY (RECENT DEVELOPMENTS)

With the discovery of the high-temperature superconductors ($T_c \geq 90K$), questions began to arise about whether or not the BCS theory sufficiently explained this new phenomenon. One of the biggest indications that it might not be sufficient was that the new samples apparently lacked any sort of an isotope effect. Recall that it was the isotope effect which led to the concept of electron-phonon interactions and hence to the BCS theory. In May and June of 1987, researchers from AT&T Bell Labs and the University of California at

Berkeley independently concluded (from experiments exchanging up to 90% O^{18} and O^{16} isotope concentrations in the sample preparations) that the isotope effect was either insignificant or completely absent [Ref. 17]. Since then, the Berkeley researchers have completed similar research varying the concentrations of copper and barium isotopic masses (Ba^{135} or Ba^{138}, and Cu^{63} or Cu^{65}) and have concluded that there is no isotope effect in the new (high-T_c) materials. Further research varying the isotopic mass of the rare earth components was not considered necessary because the critical temperature is not appreciably affected even when the rare earth is changed to a completely different rare earth. [Ref. 18]

Although no one (apparently) doubts that Cooper-pairing still plays the primary role in superconductivity, these results have caused many to doubt that phonons play the major supporting role. Indeed, as early as 1972, P. Anderson (Princeton University) and M. Cohen (U.C. Berkeley) theorized that there must be an upper limit upon temperatures at which the phonon interaction could mediate the Cooper pairing. Their argument followed the reasoning that the attractive (electron) pairing interaction was inversely proportional to the square of the phonon frequency. Therefore, continually increasing the phonon frequency (by continually raising the material's temperature) would quickly diminish the attractive pairing forces below the level of the Coulomb repulsion. The Cooper pairs would become disengaged and superconductivity quenched [Ref. 19]. To date, no one has provided a suitable theory as to which mechanism pairs the electrons in

the high-T_c materials. The theory is thus incomplete such that a summary of the factors leading to the development of the high-T_c samples might best explain the present state of thinking in the superconductivity field.

In September 1986, Bednorz and Mueller reported possible superconductivity of a percolative nature in the range of $T_c \approx 30$ K. Their breakthrough occurred in the metallic, oxygen-deficient compound $La_{5-x}Ba_xCu_5O_{5(3-y)}$ ("LBCO") with x=1 and 0.75 and y>0. Prior to arriving at this result, they had examined previous research which showed recurring evidence of superconductivity in a class of oxides known as perovskites. The point of interest was that, despite their relatively low carrier concentrations, some of these materials were shown to superconduct, albeit at relatively low T_c. This was believed to occur, under BCS theory, due to a large electron-phonon coupling. If the carrier densities at the Fermi level and the electron-phonon interactions could be enhanced in these perovskite oxides, Bednorz and Mueller felt that, under BCS theory, much higher T_cs would be possible. [Ref. 8]

One way of enhancing these effects was to follow calculations by Chakraverty in 1979 and 1981 [Refs. 20 and 21] which showed a strong relation between electron-phonon affinity and polaron formation. A polaron is a "free" electron which has confined itself in its own lattice-interaction potential well. Specifically, Chakraverty proposed that a system's ground state could readily develop a transition between superconductivity and bipolaronic-insulating states [Ref. 19].

A primary means of polaron formation is the Jahn-Teller effect [Ref. 8]. The Jahn-Teller effect describes the way in which a lattice ion lowers its energy by displacing itself within the lattice [Ref. 22]. It is this effect which contributes to the formation of structures such as the perovskite structure and which create an affinity for polaron formation. Focusing on these characteristics, Bednorz and Mueller finally arrived at the Ba-La-Cu-O system of compounds having oxygen-deficient phases and mixed-valent copper constituents with a multilayered perovskite structure. [Ref. 8]

Bednorz and Mueller manufactured their samples using an aqueous solution of nitrates (Ba-, Cu-, and La-) which they subjected to a coprecipitation process. Added to an aqueous solution of oxalic acid, a mixture of corresponding oxalates was then precipitated out of solution. The material was then heated at 900° C for 5 hours, pressed into pellets at pressure of 4 kbar and reheated to 900°C for sintering. [Ref. 8]

To provide some insight as to the structure of the material, X-ray powder diffractograms were made. These showed the existence of three distinct crystallographic phases. Only one of these phases, the layered perovskite $Ba_xLa_{2-x}CuO_{4-y}$ phase with the K_2NiF_4 structure (Figure 6), appeared to be responsible for superconductivity. By varying the sample preparation concentrations and temperature levels, they were able to examine the diffractogram intensity levels to determine the conditions required for the synthesis of each phase [Ref. 8].

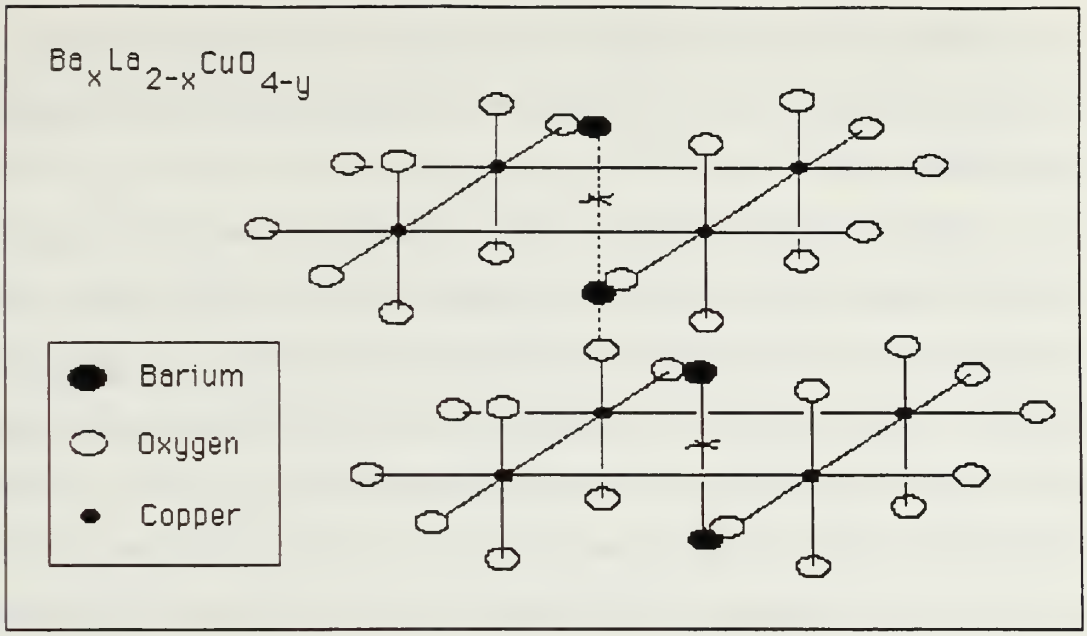

This structure consists of alternating layers along the c-axis of perovskite (CuO_3) and rock-salt (Ba-O) structures. The perovskite layers consist of corner-sharing CuO_6 octahedra. Each perovskite layer is shifted relative to the next so that the the copper sites in one layer are aligned with the oxygens in the next layer. In the CuO_6 octahedra, the Cu-O distance in the perovskite layer is smaller than the Cu-O normal to the layer. Because of the weak coupling between layers, the band structure and other properties show features associated with two dimensional behavior. [Ref. 19].

Figure 6

Tetragonal K_2NiF_4-Type Structure of $Ba_xLa_{2-x}CuO_{4-y}$

Ideally, if the existence of the non-superconducting phases were, for example, highly dependent upon barium concentrations, then altering the concentration of barium might provide a more single-phased compound.

While Bednorz and Mueller only observed complete superconductivity at temperatures in the vicinity of 13-20 K, the onset of superconductivity was clearly above 30 K. This wide spread of the transition

was later shown to be largely a function of annealing conditions which suggested that the variable valence of copper might be of significance [Ref. 23].

In late 1986, C. W. "Paul" Chu et al. (University of Houston) investigated the effects of pressure upon Bednorz and Mueller's "LBCO" compounds and found a remarkably profound effect. When they subjected their samples to a pressure of 13 kbar, they observed a shift in T_c from 32 to 40.2 K at an unprecedented rate of ~0.9 x 10^{-3} K/kbar [Ref. 24]. This result seemed to support Bednorz and Mueller's theory that superconductivity in the LBCO compounds was of a percolative, or non-bulk, nature. In their final comments, the Houston team wrote:

> The results also suggest that superconductivity at temperatures greatly exceeding 40K is achievable in LCBO and related systems through fine tuning of the sample parameters by physical and chemical means.

At the same time, R. J. Cava et al. (AT&T Bell Labs) reported observing what they concluded to be evidence of bulk superconductivity at 36K in $La_{1.8}Sr_{0.2}CuO_4$. They reported that Meissner effect measurements were 60% to 70% of the ideal value. This seemed to suggest that the granularity of the bulk material might be the reason for the apparent (in Bednorz and Mueller's work) percolative superconductivity. The grains were presumed to be bridged by Josephson coupling (electron tunneling through a superconductor-insulator-superconductor interface). They also concluded that the mechanism for this (apparent) bulk effect *could* be conventional phonon-mediated Cooper pair formation. [Ref. 23]

In early 1987, attempts to pin down the definitive explanation for the high-T_c superconductors were made more complicated by Chu's discovery of a new Y-Ba-Cu-O compound with $T_c \approx 93K$, the first material ever to superconduct above the boiling point of liquid nitrogen. Following up the results of his pressure effects experiment, Chu concluded that the superconductivity in the LBCO systems was associated with either "interfacial effects arising from mixed phases; interfaces between the metal and insulator layers, or concentration fluctuations within the K_2NiF_4 phase; strong superconducting interactions due to the mixed valence states; or yet an unidentified phase." Chu also had experimental evidence which indicated that as the LBCO compounds were made closer to a pure K_2NiF_4 phase, the onset T_c reduced and the main transition remained steady at ~37K. This combination of evidence steered him away from attempts to further purify a single K_2NiF_4 phase and turned him towards a mutiple-phase compound. [Ref. 7]

At the time of the discovery, the University of Houston group did not know what the structure of the new compound was but they did know (by X-ray diffractograms) that there were multiple phases in the compound none of which were characteristic of the K_2NiF_4 phase [Ref. 7]. Subsequent X-ray and neutron diffraction analyses (Argonne National Laboratory and others) revealed that the structure was most likely a triple layer perovskite as shown in Figure 7. There is some debate, however, over the accuracy of this structure because, in order

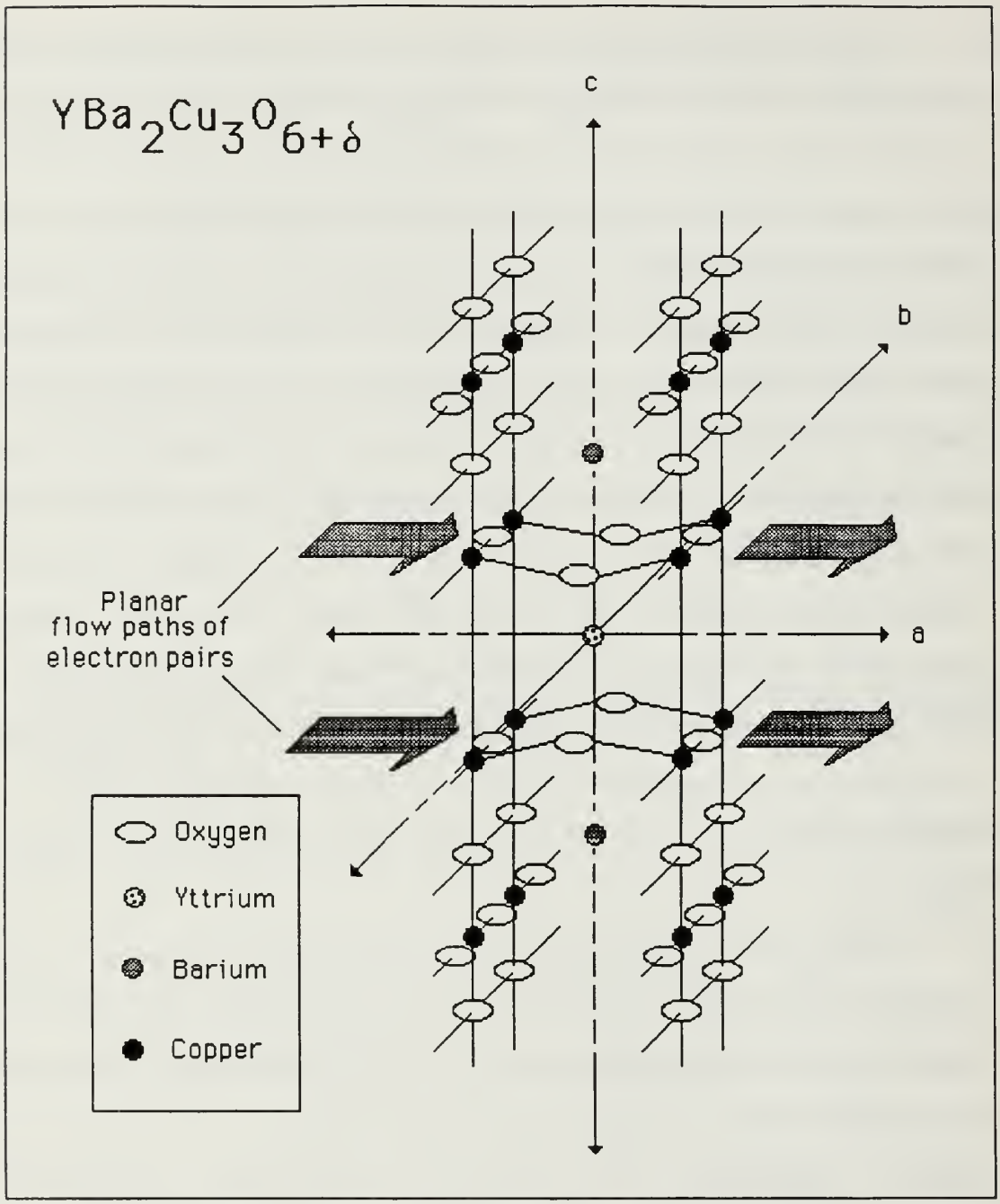

Figure 7

The Generally Accepted $YBa_2Cu_3O_{6+\delta}$ ($\delta<1$) Structure [Ref 25]

for neutron diffraction to work accurately, a pure single crystal should be used. While powder diffraction can provide accurate structure analysis, the present inability of ceramicists and crystallographers to come up with a pure single crystal of the new compounds is impeding a resolution to the debate. [Ref. 26]

Although physicists are still attempting to determine the mechanism and structures for the high-Tc superconductors, the recipe for the manufacture of these compounds is well-known and relatively simple to successfully follow. Since the discovery of the $YBa_2Cu_3O_{6+\delta}$ material,many more $T_c \approx 93K$ materials have been found by replacing yttrium with various rare earths (except Ce and Pr). Materials of this group are said to possess the single "123" phase. [Ref. 2]

Figure 7 shows, in addition to the structure, the path of the superconducting electron pairs through the lattice. The paths are confined to two-dimensional planes along the Cu-O planes bordering the yttrium atom. Varying the oxygen content during manufacture of these samples has been shown, experimentally, to decrease the critical temperature from 93K for $\delta=1$ to 55K for $.2< \delta <1$ to 20K for $\delta=.2$ [Ref. 26].

This result might suggest that T_c should drop perceptibly with only a small number of oxygen atom displacements per unit cell. One way of inducing atomic displacements in a material is to bombard that material with energtic charged particles or photons. The difficulty in displacing enough atoms to affect superconductivity is that if the new materials have percolative channels which are not damaged, even

though a bulk amount of the material is damaged, the critical temperature may remain unchanged.

C. RADIATION THEORY

When high energy electrons, such as those accelerated by a linear accelerator, encounter a macroscopic block of matter, the electrons will either pass undeflected through the matter or be scattered and possibly absorbed by the matter. In either case, the encounter is a microscopic encounter. To the electrons, which have negligible dimension in comparison to an atom, the block of matter (for a solid) is a mostly transparent geometric array of ions and electrons. While the array is mostly transparent, if a microscopic encounter does occur, the electron is quite likely to lose a large amount of energy to the particle with which it "collided." This is due to the fact that the electron has much less mass than the atomic nucleii and approximately (within a factor of the relativistic energy factor, γ) the same mass as the atomic orbital electrons of the material. If the material is bombarded with a sufficiently large number of electrons then the probability of a microscopic encounter increases accordingly. In the microscopic encounters, the bombarding electrons can excite bound electrons to different valence states, knock ions from their normal lattice sites, emit energetic photons (e.g., γ-rays and X-rays) or come to rest in the lattice [Ref. 27]. The net effect of such interactions is to alter or disrupt the order of the lattice structure which, if sufficiently distorted, can alter the "behavior" of the material. Since normal state electrical conduction is dependent upon the mean free path of free electrons in

the material, these added lattice imperfections should be evidenced by an increase in electrical resistivity; however, the factors influencing the interactions are many and the outcome is not always so readily predictable.

As the bombarding electrons travel through the target material they may lose energy such as mentioned above. The energy lost per unit path length is called the *specific energy loss*. The specific energy loss due to ionization and excitation, or *collisional losses*, can be found by an expression derived by Bethe:

$$-\left(\frac{dE}{dx}\right)_c = \frac{2\pi e^4 NZ}{m_0 v^2}\left[\ln\frac{m_0 v^2 E}{2I^2\left(1-\beta^2\right)} - \ln 2\left(2\sqrt{1-\beta^2} - 1 + \beta^2\right) + \left(1-\beta^2\right) + \frac{1}{8}\left(1-\sqrt{1-\beta^2}\right)^2\right] \qquad (6)$$

where: v ≡ electron velocity, e ≡ electron charge, N ≡ number density of absorber atoms, Z ≡ atomic number of absorber atoms, m_0 ≡ electron rest mass, I ≡ average excitation and ionization potential of the absorber, and finally β ≡ v/c the relativistic velocity ratio [Ref. 28]. This term describes the specific energy losses of lower energy electrons such as beta particles. The lower energy electrons lose energy at nearly the same rate as protons because, being of such small mass, they are quite likely to give up a large portion of their energy in just one encounter. [Ref. 29]

The large difference between electron and proton masses creates a large variation in proton versus electron specific energy losses when the electrons are accelerated to very high energies. At relativistic

velocities, the electrons are less likely to lose all their energy in just one encounter. They are more likely to be deflected through complicated scattering paths, constantly changing velocity in both speed and direction. These accelerations (or decelerations) cause the charges to radiate electro-magnetic energy in the form of bremsstrahlung radiation. The linear specific energy loss due to this radiation is described by:

$$-\left(\frac{dE}{dx}\right)_{rad} = \frac{NEZ\,(Z+1)\,e^4}{137m_0^2c^4}\left(4\ln\frac{2E}{m_0c^2} - \frac{4}{3}\right) \tag{7}$$

The radiative losses are most significant for high electron energies (E) and for absorber atoms of high atomic number (Z) due to the E and Z^2 terms in the numerator. [Ref. 28]

The average value of specific energy losses is called the *stopping power* of the absorbing material [Ref. 29]. The total linear stopping power is given by the sum of the collisional and radiative specific energy losses:

$$\frac{dE}{dx} = \left(\frac{dE}{dx}\right)_c + \left(\frac{dE}{dx}\right)_{rad} \tag{8}$$

The specific energy losses can be combined into a ratio which yields a convenient approximation:

$$\frac{\left(\frac{dE}{dx}\right)_{rad}}{\left(\frac{dE}{dx}\right)_c} \approx \frac{EZ}{700} \tag{9}$$

where E is in units of MeV [Ref. 28]. The electrons used in this experiment had an energy of 67.5 MeV and the primary absorber atom (by number density alone) was oxygen with an atomic number of 8. These values yield a ratio of 0.77 which indicates that, of the energy lost to oxygen absorber atoms, approximately 44% was radiative and 56% was collisional. The following table shows the percentages of radiative and collisional energy losses due to each absorber atom in the two superconductors:

TABLE 1

ENERGY LOSS DISTRIBUTION DUE TO RADIATION AND IONIZATION

Electron Energy: 67.5 MeV			Of energy lossed, % due to:	
Absorber Atoms	Atomic No. Z	No. Atoms / Unit Cell	Radiation	Collision/ Ionization
Yttrium	39	1	79	21
Gadolinium	64	1	86	14
Barium	56	2	84	16
Copper	29	3	74	26
Oxygen	8	~7	44	56

Giving each absorber atom a weighting value based upon its numerical distribution density in the unit cell and multiplying the weighting factor by the radiative and collisional loss percentages yields the following approximations for the distribution of energy losses:

$YBa_2Cu_3O_{6+\delta}$ ≈ 62% of energy lost is due to radiation
≈ 38% of energy lost is due to collisions/ionization

$GdBa_2Cu_3O_{6+\delta}$ ≈ 63% of energy lost is due to radiation
≈ 37% of energy lost is due to collisions/ionization.

This predominance of radiative losses may, however, be disregarded for this experiment because the sample sizes were of such small thicknesses (1.20 and 1.60 mm) that the bulk of the radiation should easily have escaped the material without further significant energy exchanges.

The specific energy loss values for these compounds' constituents can be found by interpolation of experimentally determined values for atoms as tabulated in Reference 30. Table 2 lists those interpolated values as well as the weighted values as determined by the atoms' numerical distribution density per unit cell. Summing the products of the weighted specific energy loss times ρt (the material density times the sample thickness along the beam path), for the elements in each of the compounds yields the following values of energy loss within each sample:

TABLE 2

COLLISIONAL SPECIFIC ENERGY LOSS VALUES

Absorbing Atom	Atomic No. Z	No. Atoms / Unit Cell	$(dE/dx)_c$ $\left[\frac{MeV}{g/cm^2}\right]$	Weighted $(dE/dx)_c$ $\left[\frac{MeV}{g/cm^2}\right]$
Yttrium	39	1	1.34	0.103
Gadolinium	64	1	1.20	0.092
Barium	56	2	1.23	0.189
Copper	29	3	1.44	0.332
Oxygen	8	~7	1.82	0.980

$YBa_2Cu_3O_{6+\delta}$ dEc = 2.044 MeV/electron

$GdBa_2Cu_3O_{6+\delta}$ dEc = 1.571 MeV/electron.

Multiplying these values by the electron fluence (e^-/cm^2) and the area of the irradiated surface (cm^2) results in the energy deposition within the material in units of MeV. Multiplying the MeV energy depositions by the conversion factors of 1 Joule/6.242 x 10^{12} MeV and 100 rads/(Joule/kg) yields the absorbed dose in rads. Table 3 shows these equivalent doses for each sample. These rad doses will be used later in the Results section to compare to both the Lockheed team experiment with gamma radiation [Ref. 2] and the Naval Research Laboratory team experiment with 56 MeV electron irradiation [Ref. 1].

TABLE 3

ELECTRON FLUENCES TO ABSORBED DOSE EQUIVALENCIES

E_{e^-} = 67.5 MeV	Absorbed Radiation Dose [rads]	
Electron Fluence [e^-/cm^2]	$YBa_2Cu_3O_{6+\delta}$	$GdBa_2Cu_3O_{6+\delta}$
10^{13}	2.99×10^5	3.17×10^5
10^{14}	2.99×10^6	3.17×10^6
10^{15}	2.99×10^7	3.17×10^7
5×10^{15}	1.49×10^8	1.59×10^8

III. EXPERIMENTAL PROCEDURES

A. RADIATION FACILITY

Irradiations were performed using the electron linear accelerator, or LINAC, at the U.S. Naval Postgraduate School in Monterey, California. The LINAC is a pulsed-beam (electron), travelling-wave accelerator capable of producing up to 120 MeV electrons with an average beam current of 1.0 mamps. The accelerator section is comprised of three ten-foot circular waveguide sections. Each ten-foot section is "driven" by its own twenty-two megawatt klystron amplifier which feeds RF energy into that section. The evacuated waveguide structure has internal copper loading disks which slow the phase velocity of the RF wave to the speed of light, which in turn provide a mechanism by which the electron bunches, "riding" on the crests of the RF wave, can be accelerated to relativistic energies.

The electrons are produced by a thermionically emitting electron gun at the beginning of the waveguide. The electrons are pulsed, or bunched, to a pulse length of 1.0 μseconds and a repetition rate of 60 Hz. The electron bunches are injected into the first accelerator section with an energy of approximately 80 KeV and those with the proper phase relation will be accelerated by the RF waves. Each klystron section can impart approximately 35 MeV of energy to the electron beam. In this experiment, the last klystron was left

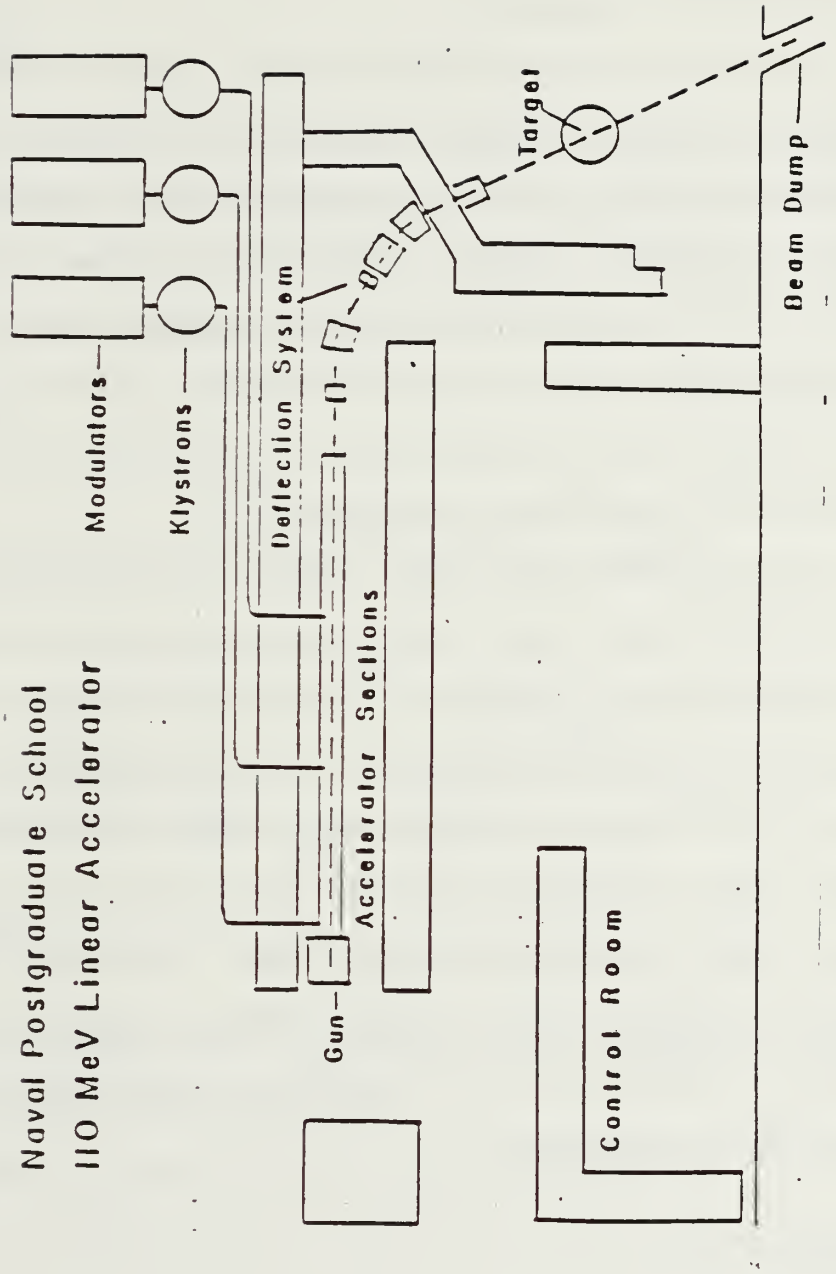

Figure 8

Naval Postgraduate School Linear Accelerator

inactive and the beam was tuned to an energy of 67.5 MeV. The maximum beam current used during this experiment was approximately 3.0×10^{-6} amperes.

At the end of each klystron section, the RF energy is dumped, leaving only the relativistic electrons to continue. After the third accelerator section, the electrons pass through a beam collimator and enter the deflection system. The deflection system consists of two 30 degree bending magnets, an energy defining slit, two quadrupole focusing magnets and two sets of Helmholtz coils for aiming the beam. The focused beam then passes into the target area and is finally terminated in an underground beam dump field.

Although the LINAC has a maximum electron pulse capacity of 1011 electrons per pulse, a more accurate method of measuring electron beam fluence employs a Secondary Emissions Monitor (SEM) placed in the path of the beam. In this experiment the SEM was placed in the beam downstream of the target. The SEM employs a foil which emits secondary electrons when impacted by the incident beam. These secondary electrons charge, and thereby create a voltage across, a capacitor. This voltage, which is determined by a voltage integrator connected to the capacitor, is proportional to the stored charge by the relationship:

$$Q_{SEM} = C\,V \tag{10}$$

where Q_{SEM} is the charge on the capacitor, C is the capacitance, and V is the integrated voltage. To find the number of electrons the SEM

detected, N_{SEM}, divide the charge, Q_{SEM}, by the charge per electron, e:

$$N_{SEM} = \frac{CV}{e} \tag{11}$$

The SEM calibration, done previously against a Faraday cup, revealed that the efficiency of the SEM in detecting electrons is 6.1 percent [Ref. 31]. This implies that the total number of electrons, N, passing through the SEM, and hence the target, is:

$$N = \frac{N_{SEM}}{.061} \tag{12}$$

The electron fluence, Φ, is then defined by the relation:

$$\Phi = \frac{N}{A} \tag{13}$$

where A is the cross-sectional area of the electron beam. Combining equations (10) through (13) yields:

$$\Phi = \frac{CV}{(.061)eA} \tag{14}$$

which is the relation used to determine LINAC settings to obtain the desired fluences in this experiment.

The initial, generally held belief that superconductivity in the $RBa_2Cu_3O_{7-x}$ compounds was strongly dependent upon the positioning of the oxygen atoms (and their vacancies) [Ref. 25] created some concern that high energy irradiation in a vacuum might affect the surface

layer oxygen concentrations. Furthermore, as later became apparent, there was concern that the compounds might be susceptible to damage from unnecessary exposure to moisture in atmospheric air. For these reasons, and in an effort to assimilate conditions in some earlier gamma ray irradiation experiments, an argon atmosphere was selected for irradiation and storage/transport. The small size and the brittleness of the provided samples made stabilizing them for radiation difficult and therefore excluded the feasibility of passing a bath of argon across the sample during irradiation. While it did not permit a 100-percent argon atmosphere, the plexiglass chamber shown below provided the best overall solution to the aforementioned concerns.

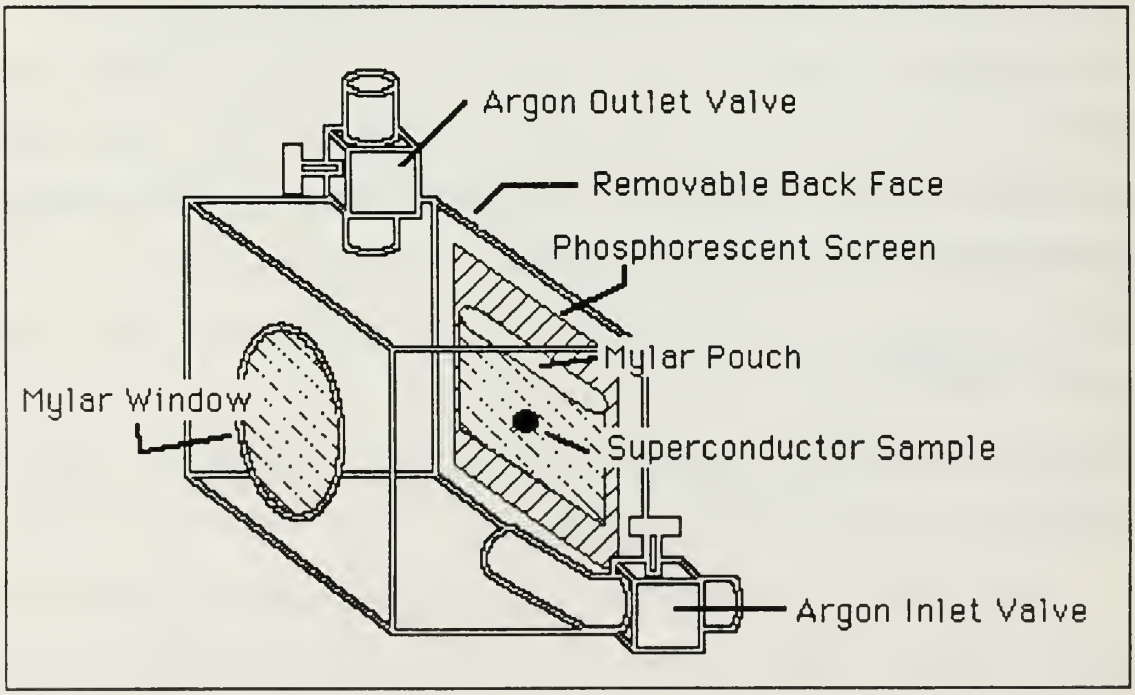

Figure 9

Argon Chamber for Irradiation of Superconductor Samples

Prior to installing the sample, the empty chamber was placed in its marked position in the LINAC target area. The beam was then turned on, centered, and focused to the desired size (2 cm^2 circle drawn in center of phosphorescent screen) from the control room where it was observed via a remote video display. This was done to eliminate any adjustments of the beam when the sample was installed which might have otherwise introduced considerable error in the smaller fluences. Once these adjustments were completed, the beam was turned off and the sample was positioned in the mylar pouch so it was precisely centered on the front side (uncoated) of the phosphorescent screen. The back of the chamber was then screwed back on, creating an air tight seal against its rubber gasket. Both air valves were then throttled slightly open and argon at approximately 2 p.s.i. was introduced through the inlet. The argon was permitted to flow in the bottom of the chamber slowly in order to displace the lighter air out through the top. Being careful not to over-pressurize, which would rupture the mylar window on the front wall of the chamber, the exhaust valve was closed followed immediately by the inlet valve. The chamber was then placed precisely back in its marked position and the beam turned back on. Upon reaching the desired integrated voltage as determined by equation (14), the beam was shut down and the sample (more significantly, the plexiglass chamber) was monitored for radioactivity. Once safe levels were verified, the sample was placed back into its transportation chamber, which was then charged with 2 p.s.i. argon.

B. RESISTANCE MEASURING FACILITY

Since the LINAC facility and the measurement laboratory (Lockheed Missile and Aerospace, Palo Alto, California) were, by car, approximately two hours apart, annealling time was considerable. In an effort to minimize this logistically imposed problem, the measurements were always performed the same day as the irradiations. An additional contributor to annealing time was the length of time required in preparing the sample for measurement. As previously discussed, the AC four-probe method was employed for measuring the resistances of the samples. Since the samples were less than 5.0 millimeters across and since the platinum leads were nearly imperceptible to the naked eye, soldering (indium solder) the leads to the wires in the helitrans (cooling chamber assembly) tray required the use of a microscope. With the leads in such close proximity to one another, the heat of the soldering iron frequently caused adjacent previously soldered connections to melt apart. Furthermore, transportation and handling of the samples occasionally caused the pressed indium connection sites on the samples to come loose. Reconnecting these contacts added considerable time to the already high annealing time.

Once all connections were made and tested for continuity, the helitrans tray was inserted into its refrigeration shield. Continuity was again checked to ensure the shield provided no ground to any of the leads. The helitrans assembly was then roughed out to a vacuum of approximately 200-400 torr, then drawn to a vacuum of approximately 10^{-5} torr using an ion diffusion pump. The evacuated heliarc assembly

was then placed into its stand and connected to the liquid helium line and the measuring equipment as shown in Figures 10 and 11.

The setup shown utilized a lock-in amplifier to maintain a proper phase relationship between the voltage measurements and the 100 Hz AC current source. This eliminated much of the noise which may have otherwise been present. Two thermocouples were necessary (a) in order to monitor the superconductor samples' temperature and (b) to monitor the temperature of the tip of the liquid helium nozzle in the helitrans. This was useful in controlling the temperature change rate by adjusting the liquid helium flow. Each sample's resistances were measured as follows:

1. From 300K to about 80K on a small scale to show the critical temperature and to display any anomalies which might emerge.
2. From about 80K to about 105K (and back again) on a large scale to display the transition region for closer analysis.
3. Any anomalies discovered in the previous two measurements were again repeated on large scales for closer analysis.

Upon completion of one sample, the system was set up for the second sample and the process repeated.

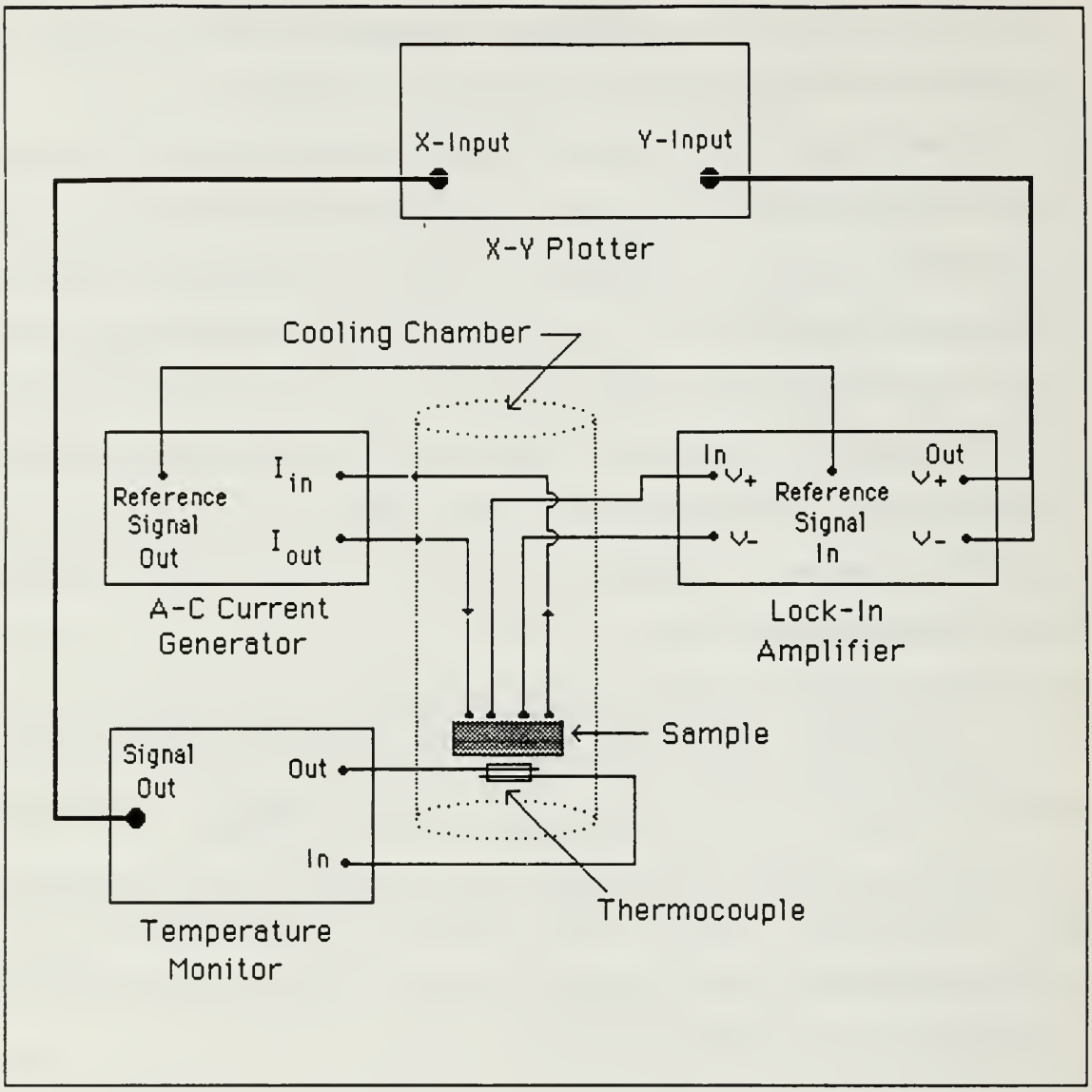

Figure 10

General Circuit Diagram for R-T Measurements Using A-C Four-Probe method.

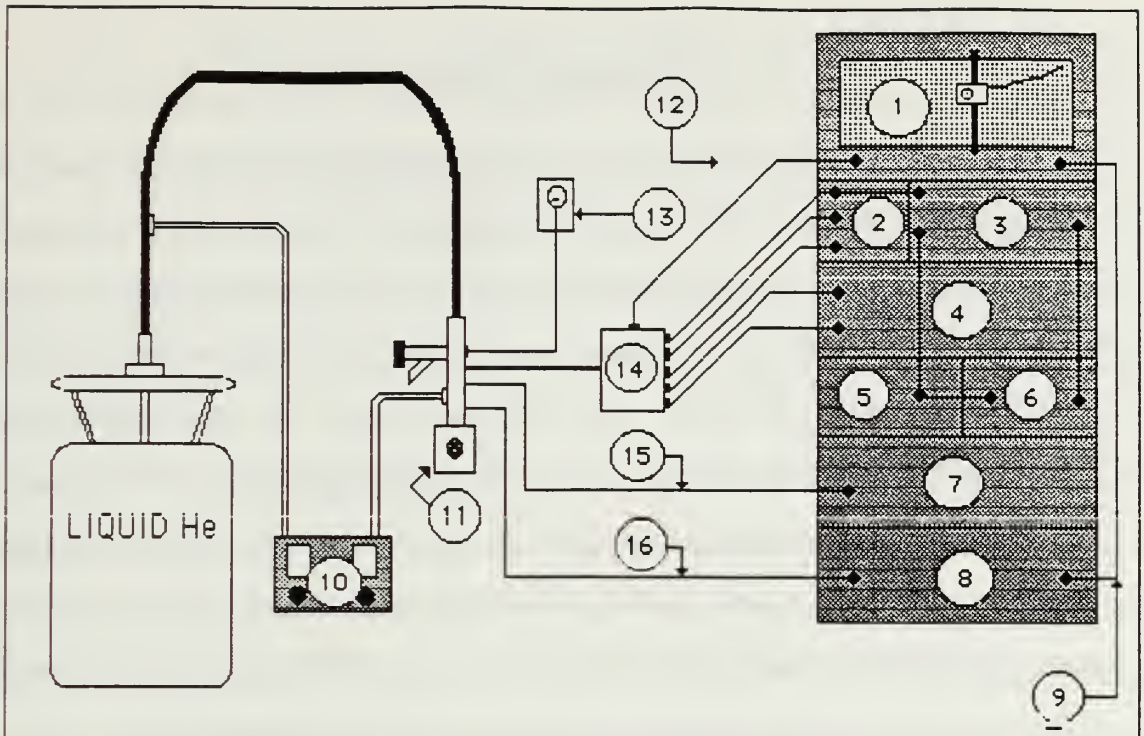

1. X-Y Plotter
2. Differential Pre-Amp, EG&G Princeton Applied Research Model 5316.
3. Lock-In Amplifier, EG&G Princeton Applied Research Model 5301.
4. Differential Pre-Amp, EG&G Princeton Applied Research Model 116.
5. Current Amplifier, Keithly Model 427.
6. Current Monitor, Data Precision 3600.
7. Digital Temperature Indicator/Controller (Helitrans heater temperature), Air Products.
8. Digital Temperature Indicator/Controller (Helitrans cold plate temperature), Air Products.
9. Helitrans Cold Plate (and superconductor sample) Temperature Input to X-Y Plotter.
10. Liquid He Flow Controller, Air Products.
11. Evacuated Helitrans Sample Cooling/Mounting Tray.
12. Superconductor Measured Voltage Input to X-Y Plotter.
13. Helitrans Heater Power Cord/Source (110V AC).
14. Sample Measurement Switch Box.
15. Helitrans Heater Thermocouple.
16. Helitrans Cold Plate Thermocouple.

Figure 11

Resistance vs. Temperature Measuring Laboratory Setup

IV. EXPERIMENTAL RESULTS

Superconducting $YBa_2Cu_3O_{6+\delta}$ and $GdBa_2Cu_3O_{6+\delta}$ compound samples, both with T_c = 92K, $\delta \leq 1$ and prepared at University of Houston, were used in this experiment. Previous X-ray diffractograms verified that both the samples possessed only the "123" single phase [Ref. 2]. The $YBa_2Cu_3O_{6+\delta}$ sample's dimensions (Figure 12) were: L=4.75mm, t=1.60mm and d=2.00mm. The dimensions of the $GdBa_2Cu_3O_{6+\delta}$ sample were approximately L=5.26mm, t=1.18mm and d=2.5mm. Both samples were irradiated with the beam normal (or nearly so) to their top semicircular faces so that the undeflected beam path through the material was approximately equal to the thickness, t.

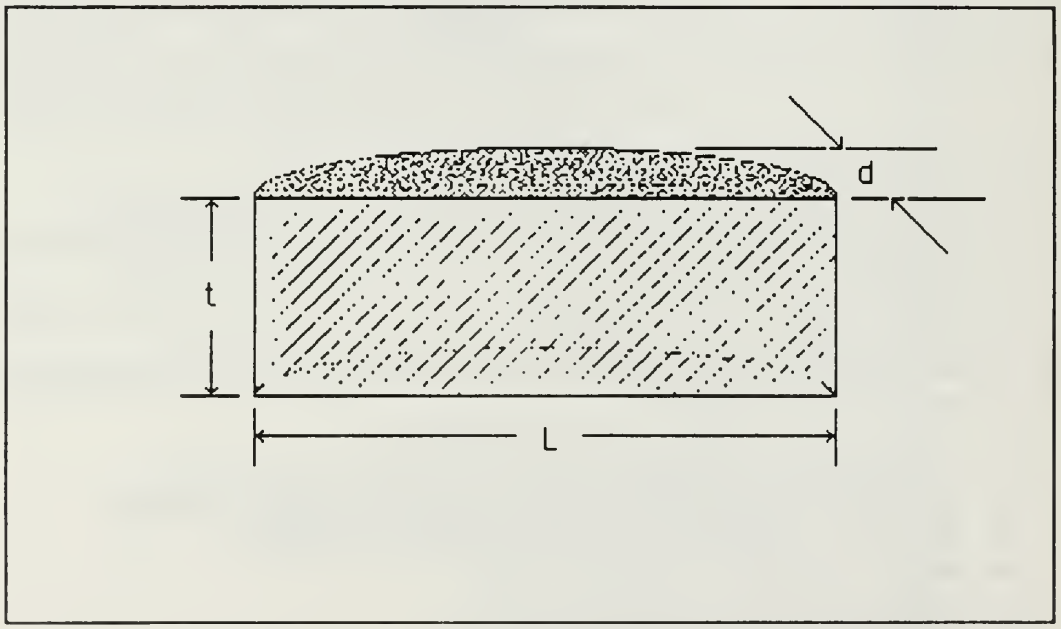

Figure 12

Dimensions of Irradiated Superconductor Samples

Each sample was exposed to a series of 67.5 MeV electron irradiation doses with each irradiation followed by a two to five hour annealing time (logistically-imposed) and measured for resistance versus temperature dependence from room temperature (300K) to about 10-15 K into the superconducting region (~80K) using the A-C four-probe method previously described in the section on superconductor theory.

The $YBa_2Cu_3O_{6+\delta}$ sample showed a drop in resistance in the normal state after each electron irradiation, until a fluence of 10^{14} electrons/cm^2 was reached. Afterwards, the normal state resistances increased slightly (Figures 13-17 and 23); however, the $YBa_2Cu_3O_{6+\delta}$ sample had become quite crumbly in the vicinity of the pressed indium contacts by this stage of the experiment and the contacts frequently pulled out of the sample. While every attempt was made to keep the contacts in the same locations in the sample, at a fluence of 10^{14} electrons/cm^2 (~3 Mrads exposure) it became necessary to relocate one of the voltage lead connections. This relocation may have changed the conduction path distances between voltage probes sufficiently to vary the resistance readings accordingly. The $GdBa_2Cu_3O_{6+\delta}$ sample showed very little change in normal state resistance until the final fluence of $5X10^{15}$ electrons/cm^2 (~150 Mrads exposure) where it showed a considerable drop (Figures 18-22 and 24). This was the first time that the $GdBa_2Cu_3O_{6+\delta}$ sample displayed crumbling in the

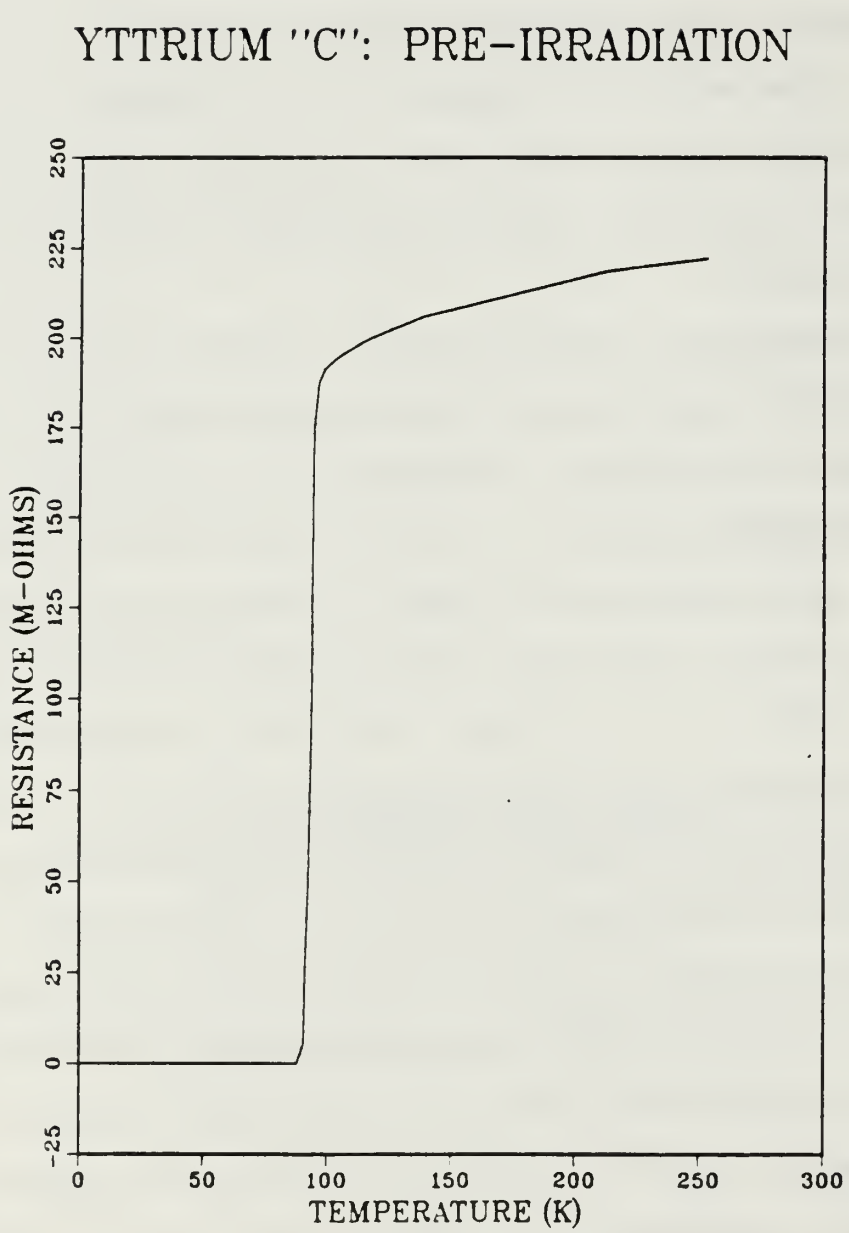

Figure 13

Resistance (mΩ) vs. Temperature (K) Plot of $YBa_2Cu_3O_{6+\delta}$ Prior to Irradiation

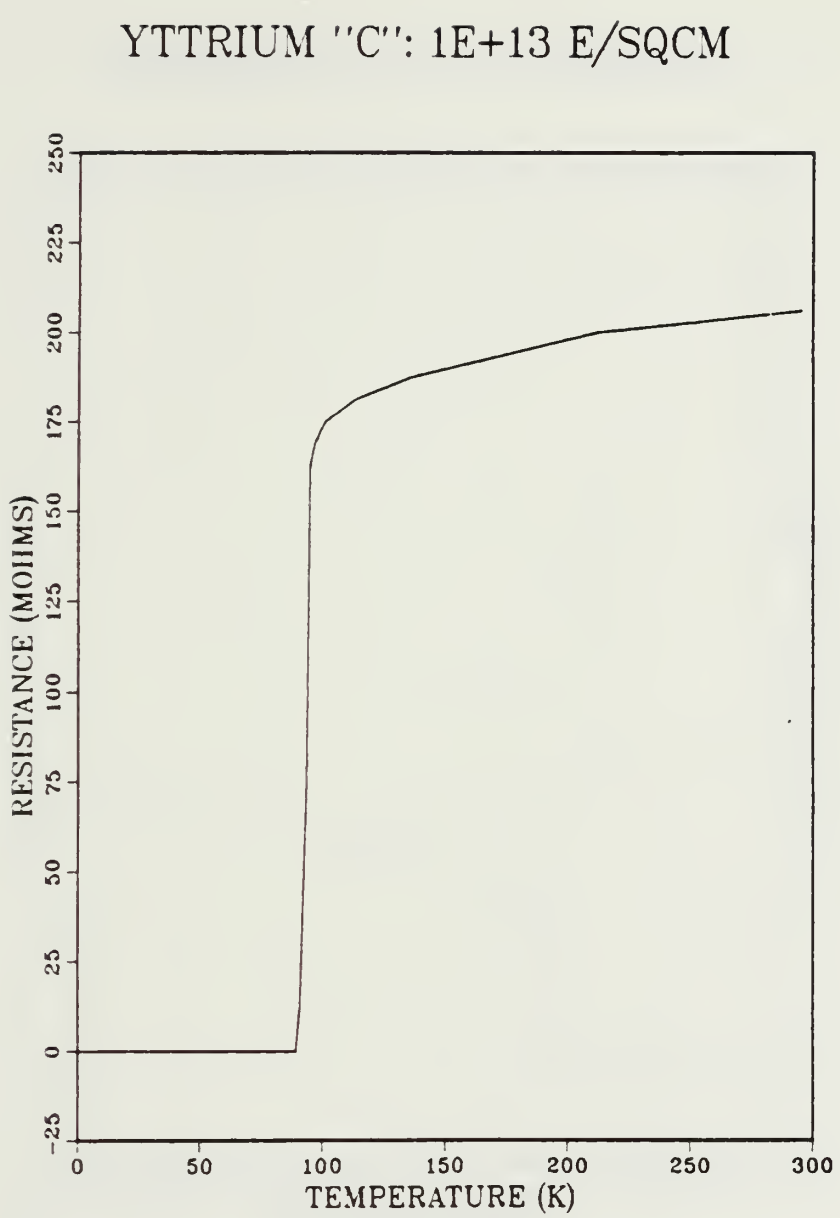

Figure 14

Resistance (mΩ) vs. Temperature (K) Plot of $YBa_2Cu_3O_{6+\delta}$ after 10^{13} Electron/cm^2 Fluence (0.3 Mrad Exposure)

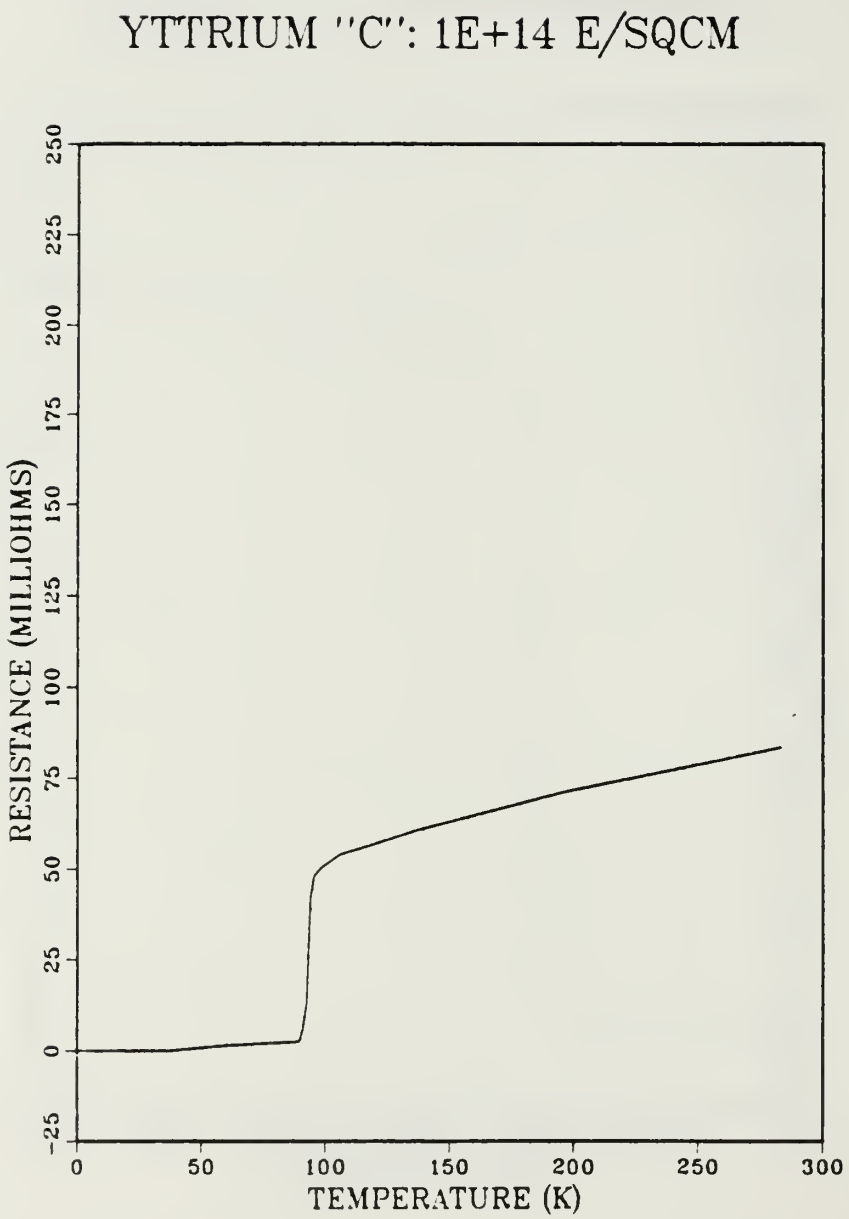

Figure 15

Resistance (mΩ) vs. Temperature (K) plot of $YBa_2Cu_3O_{6+\delta}$ After 10^{14} Electrons/cm^2 Fluence (3 Mrad exposure)

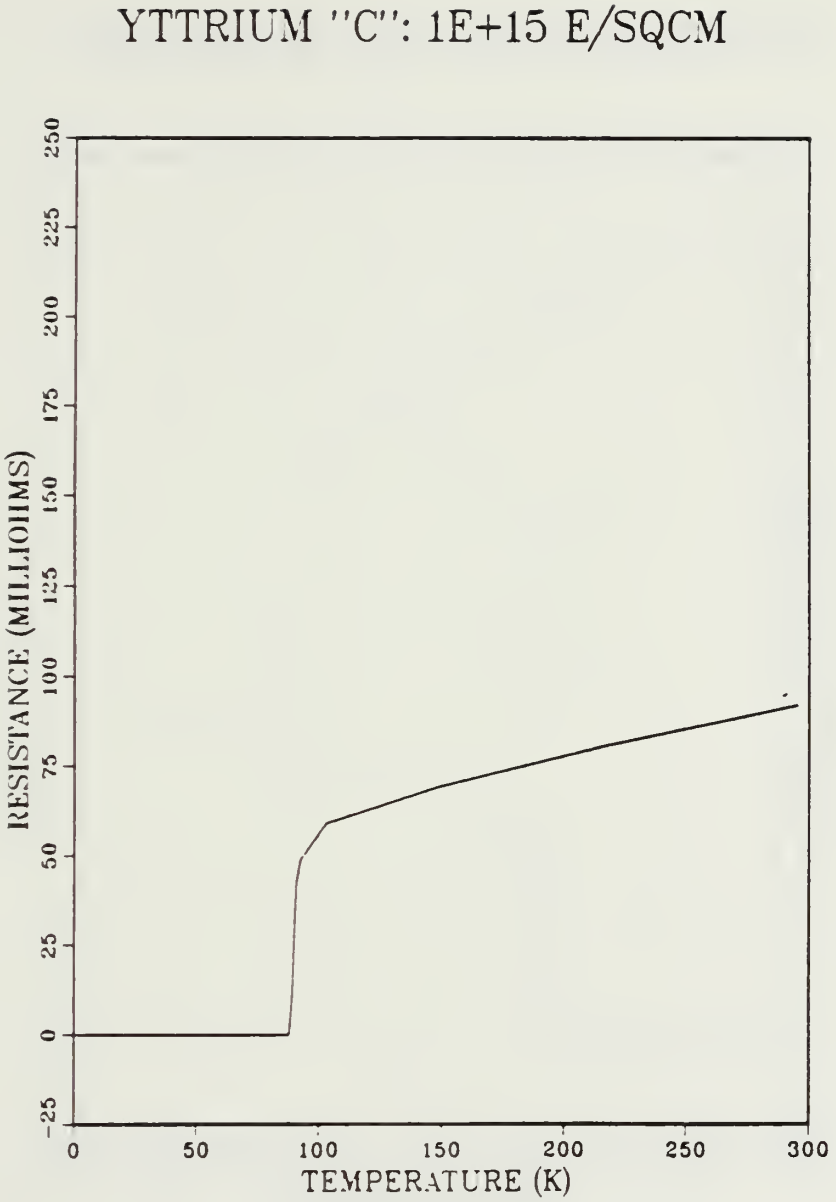

Figure 16

Resistance (mΩ) vs. Temperature (K) Plot of $YBa_2Cu_3O_{6+\delta}$ After 10^{15} Electrons/cm^2 Fluence (30 Mrad Exposure)

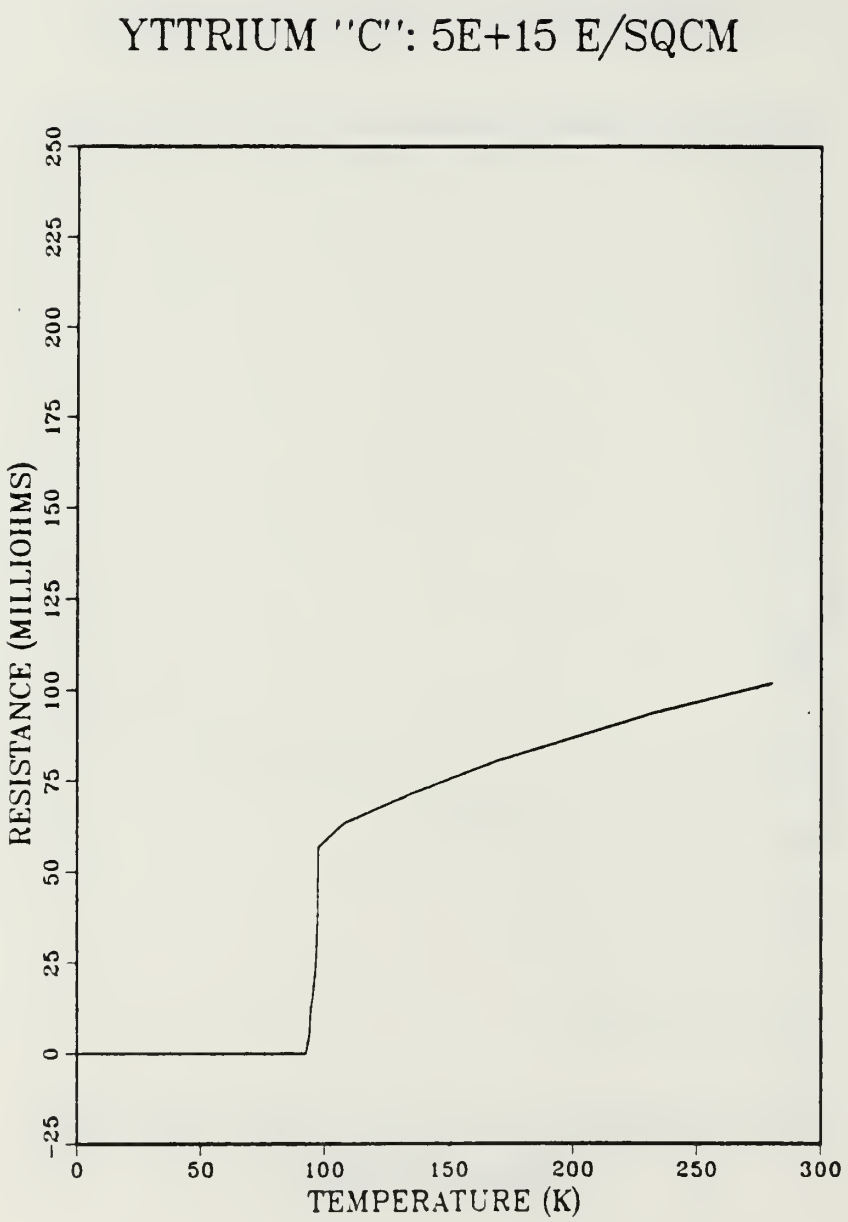

Figure 17

Resistance (mΩ) vs. Temperature (K) Plot of $YBa_2Cu_3O_{6+\delta}$ After $5x10^{15}$ Electrons/cm^2 Fluence (150 Mrad Exposure)

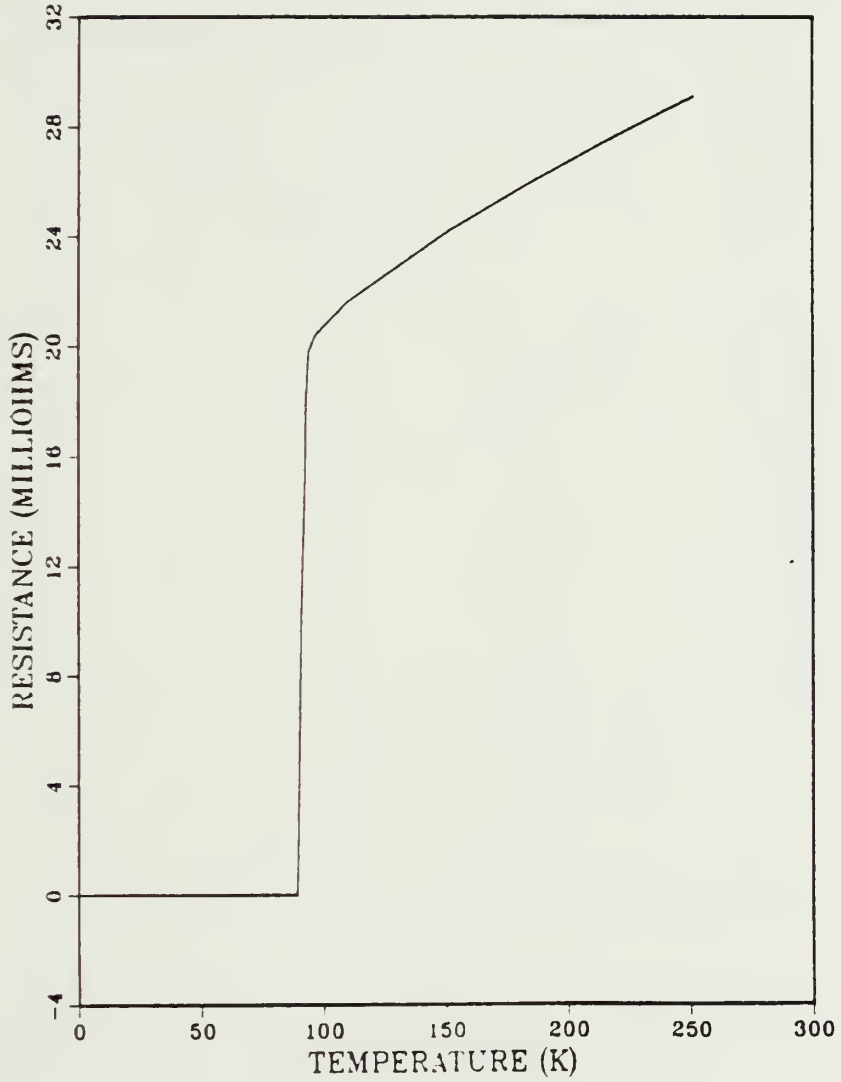

Figure 18

Resistance (mΩ) vs. Temperature (K) Plot of $GdBa_2Cu_3O_{6+\delta}$ Prior to Irradiation

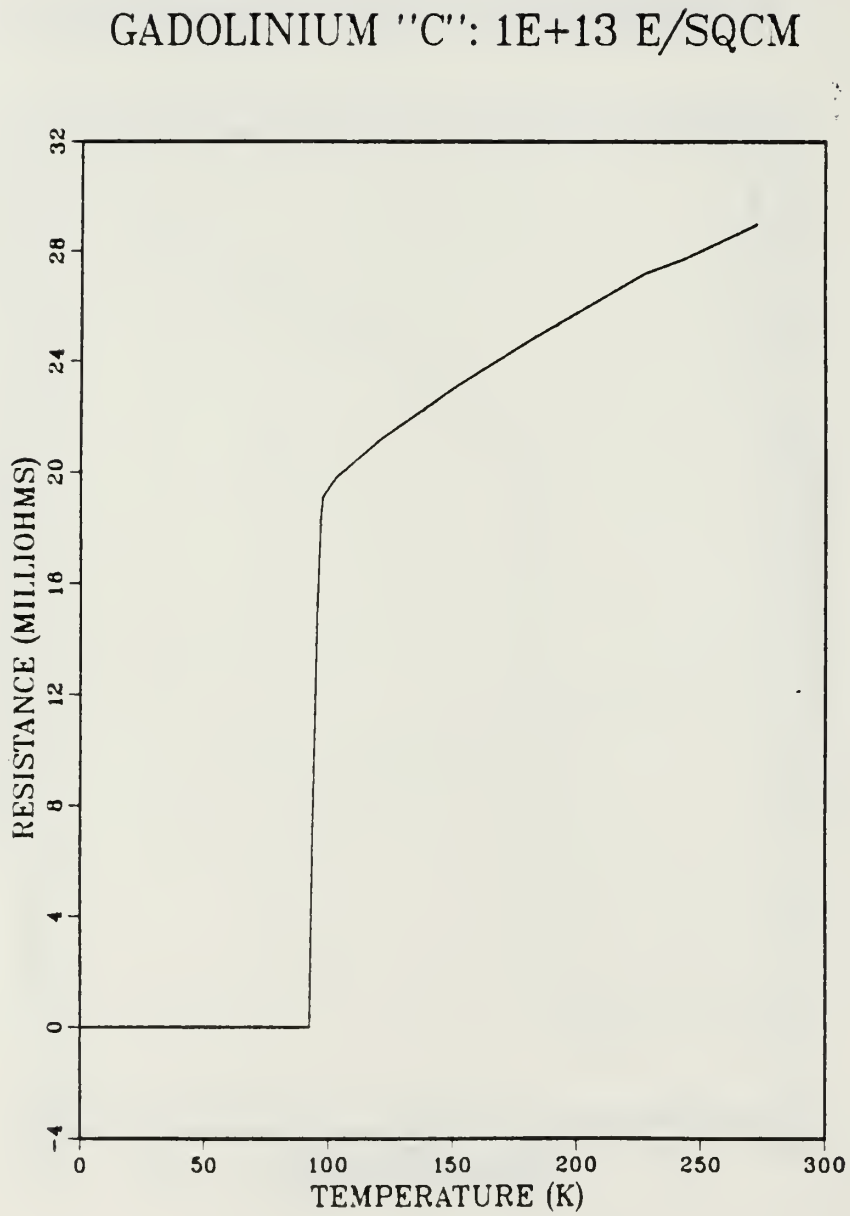

Figure 19

Resistance (mΩ) vs. Temperature (K) Plot of $GdBa_2Cu_3O_{6+\delta}$ After 10^{13} Electrons/cm^2 Fluence (0.3 Mrad Exposure)

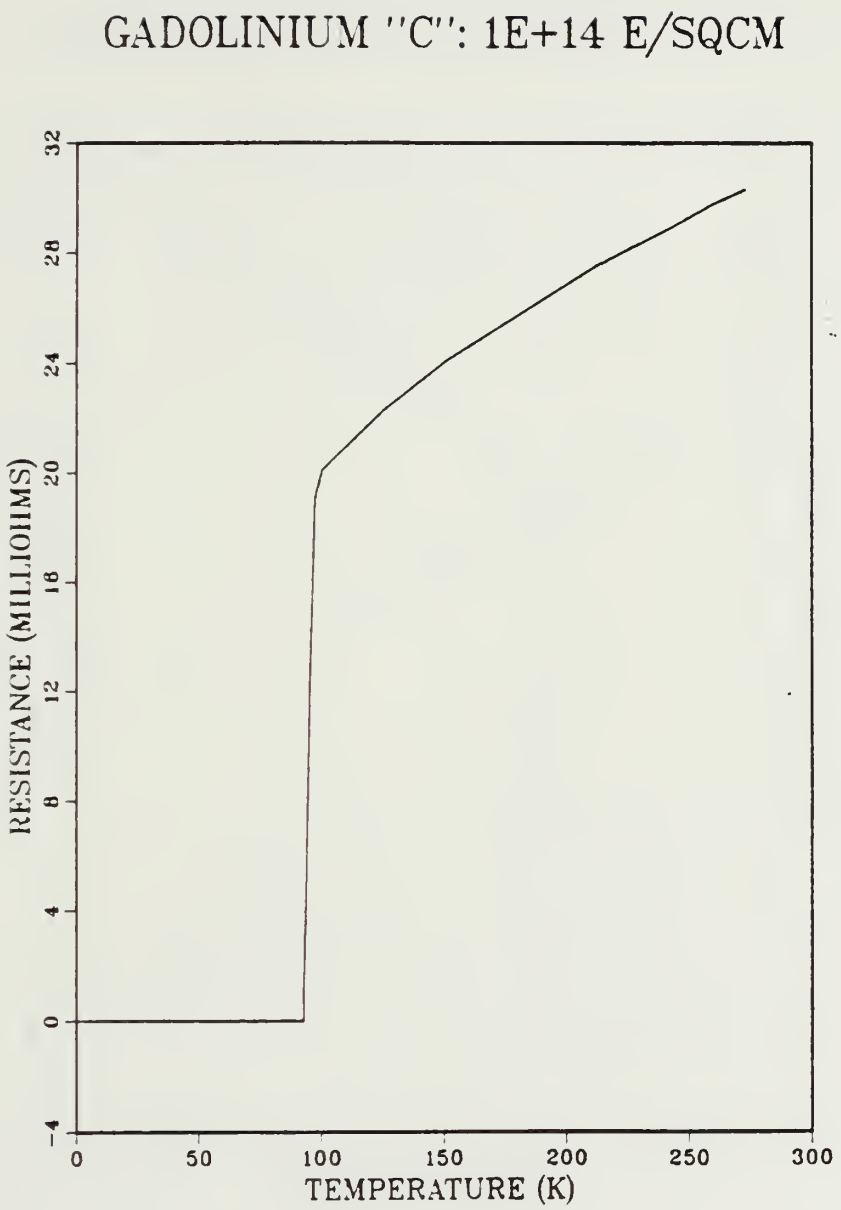

Figure 20

Resistance (mΩ) vs. Temperature (K) Plot of $GdBa_2Cu_3O_{6+\delta}$ After 10^{14} Electrons/cm^2 Fluence (3 Mrad Exposure)

Figure 21

Resistance (mΩ) vs. Temperature (K) Plot of $GdBa_2Cu_3O_{6+\delta}$ After 10^{15} Electrons/cm^2 Fluence (30 Mrad Exposure)

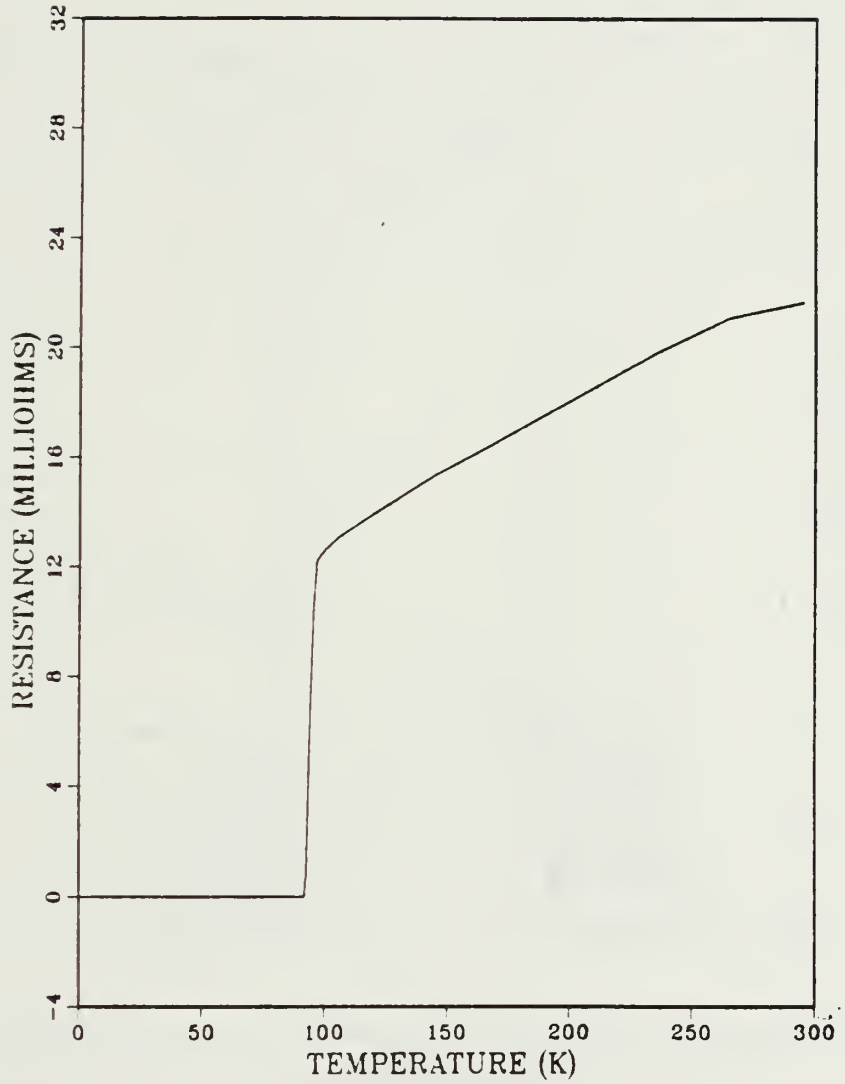

Figure 22

Resistance (mΩ) vs. Temperature (K) Plot of $GdBa_2Cu_3O_{6+\delta}$ After $5x10^{15}$ Electrons/cm^2 Fluence (150 Mrad Exposure)

YTTRIUM "C"

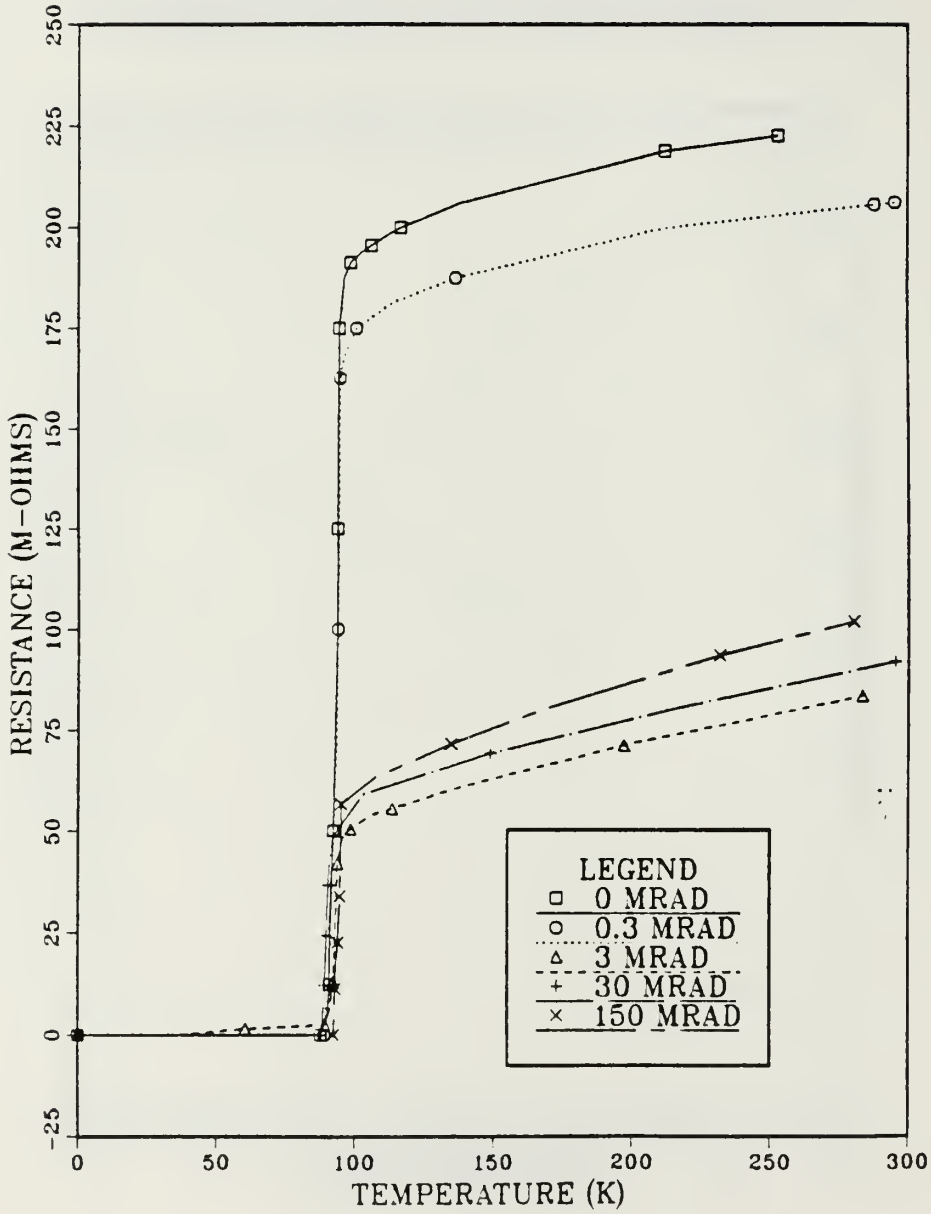

Figure 23

Composite Resistance (mΩ) vs. Temperature (K) Plot of $YBa_2Cu_3O_{6+\delta}$ for Pre-irradiation and All Subsequent Irradiations

GADOLINIUM "C"

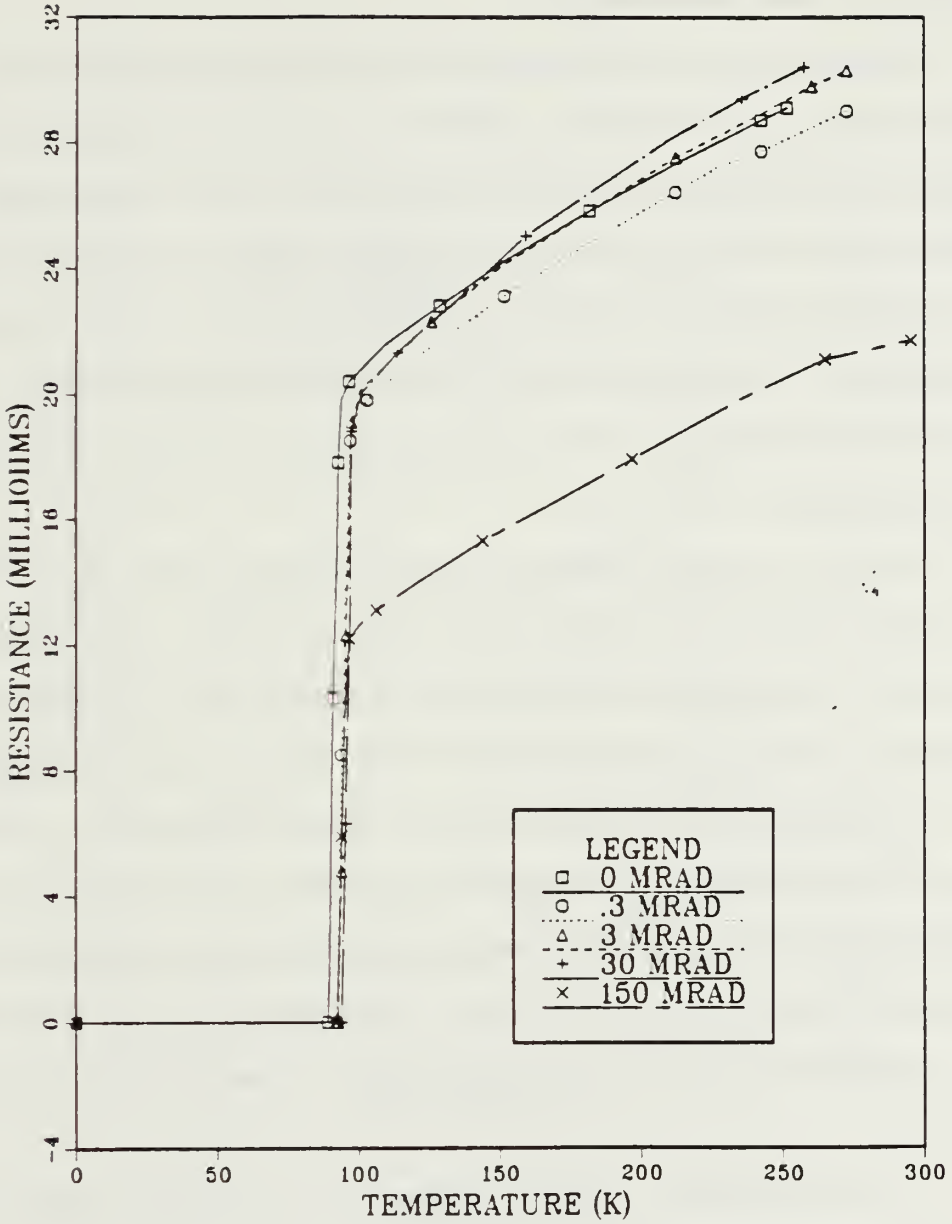

Figure 24

Composite Resistance (mΩ) vs. Temperature (K) Plot of $GdBa_2Cu_3O_{6+\delta}$ for Pre-irradiation and All Subsequent Irradiations

vicinity of the contacts. Here, as with the YBa2Cu3O6+d sample, the pressed indium contact was slightly relocated and the resistance showed a considerable change.

Transition region effects appeared primarily in the form of slight variations in the transition slopes in both the $YBa_2Cu_3O_{6+\delta}$ and $GdBa_2Cu_3O_{6+\delta}$ samples (Figures 23 and 24). These were similar to the slight effects seen by the Lockheed group [Ref. 2]; however, there was no apparent trend to these fluctuations, and they may, therefore, be attributable to slight variations of the sample locations within the helitrans tray (in relation to the thermocouple) for each of the resistance measurements.

A more dramatic transition effect occurred after the 10^{14} electron/cm^2 irradiation of the $YBa_2Cu_3O_{6+\delta}$ sample. The onset of the transition occurred at approximately 98.4K and continued dropping typically until approximately 88.6K where the slope suddenly "tailed off" at a resistance of approximately 2.5 mW (Figure 25). The resistance did not vanish until approximately 24K. This measurement was repeated three times without any change in results. Surprisingly, the effect did not repeat itself in any of the subsequent irradiations. It only appeared for the 10^{14} electron/cm^2 irradiation and vanished for the rest.

The $YBa_2Cu_3O_{6+\delta}$ sample exhibited more obvious signs of structural deterioration throughout the experiment than did the $GdBa_2Cu_3O_{6+\delta}$ sample. This was observed under optical microscope

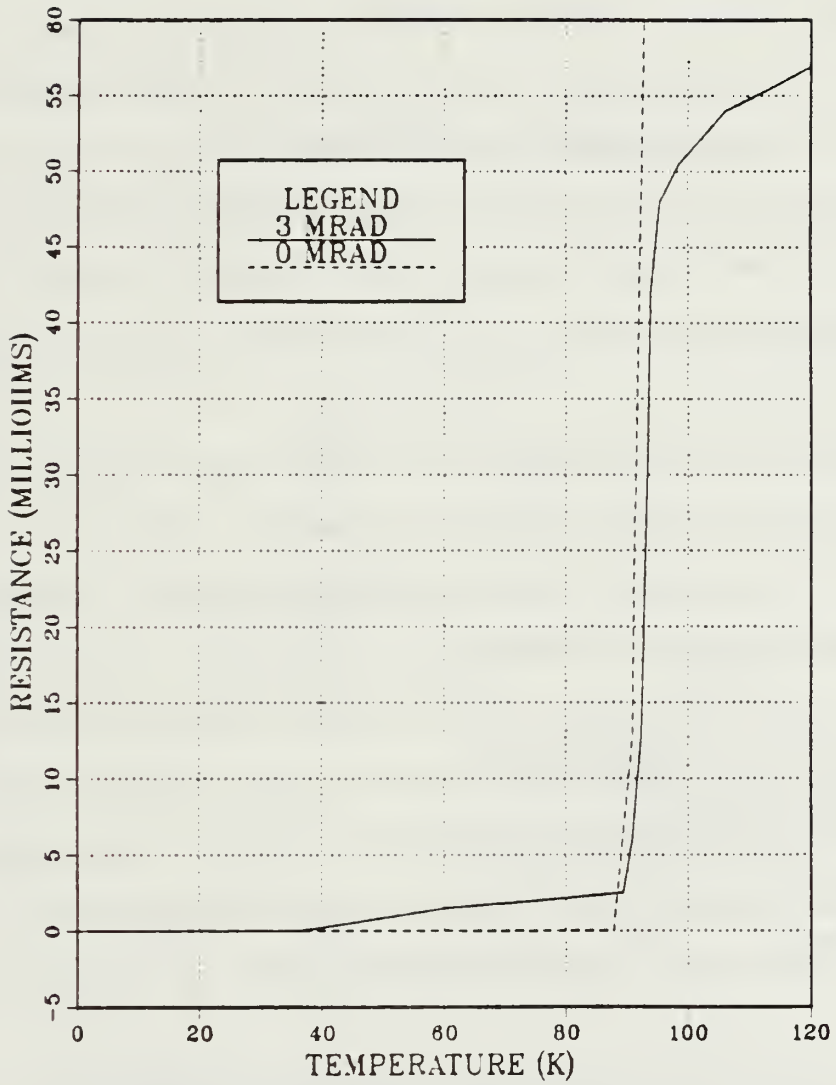

Figure 25

Large-Scale Resistance (mΩ) vs. Temperature (K) Plot of $YBa_2Cu_3O_{6+\delta}$ After 10^{14} Electrons/cm^2 Fluence (Solid Curve) and Pre-Irradiation Sample(DashedCurve)to Examine Failure to Achieve Zero Resistance Above 77K

examination and was evidenced by the difficulties in getting the indium contacts to take hold in the $YBa_2Cu_3O_{6+\delta}$ sample. The superconductor material in the vicinity of the contacts became very crumbly and the presssed indium contacts consequently came loose. The problem was analogous to the difficulty one might encounter in getting a piece of gum to stick to a dirty surface—the gum would stick well to the dirt, but the least amount of pull would separate the dirt from the surface. The $GdBa_2Cu_3O_{6+\delta}$ sample appeared to better maintain its structural integrity with very few contact problems until the last irradiation.

Figures 26 and 27 show the results of the Lockheed gamma irradiations and the NRL electron irradiations, respectively, in comparison to the applicable data from this experiment. In Figure 31, the plots are normalized by setting the unirradiated sample resistances to unity at 290 K. The only data from this experiment plotted in Figure 26 are for the unirradiated and 0.3 Mrad exposure measurements. This is due to the aforementioned relocation of the indium contact before the measurements following the 3 Mrad exposure. All subsequent data would therefore be meaningless in this normalized comparison.

In Figure 27, the plots are normalized by setting the 3 Mrad (this experiment) and the 1 Mrad (NRL experiment) resistances to unity at 290 K (Note: equating the two with an exposure difference of 2 Mrad should be acceptable since Reference 1 indicated there was no

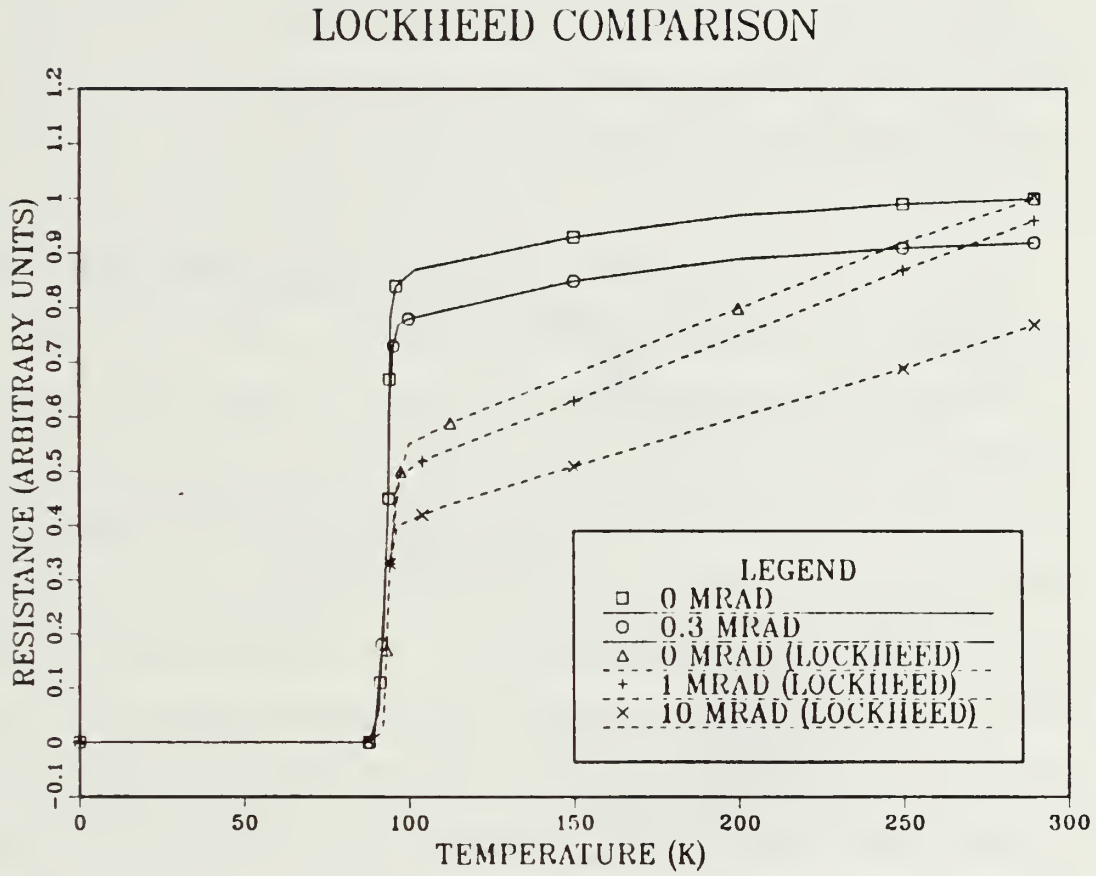

All curves normalized by setting pre-irradiated resistances to unity at 290 K.

Figure 26

Resistance (mΩ) vs. Temperature (K) Plot of $YBa_2Cu_3O_{6+\delta}$ Data From This Experiment Compared to Data for Similar Compound From Lockheed Experiment (Gamma Irradiation) [Ref. 2]

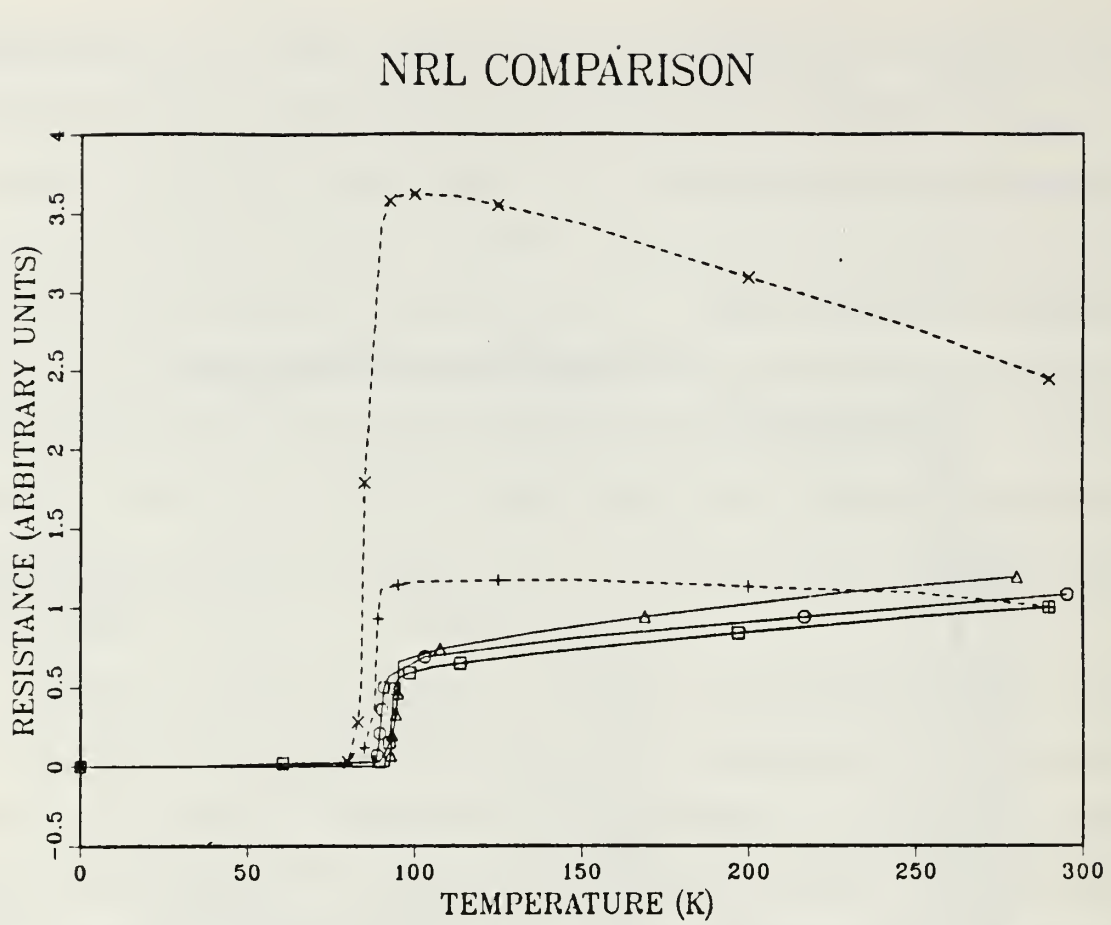

Figure 27

Resistance (mΩ) vs. Temperature (K) Plot of $YBa_2Cu_3O_{6+\delta}$ Data From This Experiment Compared to Data for Similar Compound in 100μm Thick Film from NRL Experiment (Electron Irradiation) [Ref. 2]

appreciable difference in data within the lower irradiation exposures). The only data plotted in Figure 27 from this experiment are for the 3, 30, and 150 Mrad exposures. This is because, even though the platinum leads were jostled and even moved slightly within the indium at times, the indium connections were not relocated again.

The results of this experiment were similar to the Lockheed results in that the normal state resistances dropped with increasing irradiations. Furthermore, the same measuring apparatus was used for each experiment. This might explain the similarity of broadening in the transition region with the lack of a discernable trend.

The NRL results, although conducted similarly (fluences and energies were within 15 percent between experiments; however, the NRL study involved 100mm thick films as opposed to bulk samples) differed markedly. The NRL normal state resistances increased considerably with increasing irradiation and showed a continuous rise with decreasing temperature in the vicinity of the transition. No such rise in the transition region of the normal state was observed in any of this experiment's measurements. This rise near the transition was prevalent in nearly all of the early (i.e., Bednorz and Mueller's La-Ba-Cu-O compounds) high-temperature superconductors, and the steepness of the rise was generally a function of the annealing atmosphere's oxygen content. Although NRL's compounds were of a different structure, perhaps a parallel can be drawn to suggest that oxygen atoms were displaced in the 100 Mrad case.

Neither team reported macroscopic indications of crumbling and wire lead connection difficulties such as observed in this experiment. This could be due to the number of times (~10 times each) the samples in this experiment were cycled through the range of temperatures spanning a range of over 200-K. If the indium contacts had a different thermal expansion rate, then the stresses created during thermal cycling may well have been sufficient to crumble the structure in the vicinity of those contacts. Furthermore, moisture has already been determined to be detrimental to these compounds and the numerous hours under the microscope (to attach the wire leads for measurements) may have subjected the samples to condensation from moisture in the atmosphere and condensation from the operator breathing while working necessarily close to the samples. Of course, this crumbling may also be an irradiation effect, but its localization in the vicinity of the indium contacts suggests more convincingly that the thermal expansions are the cause.

In summary, the $GdBa_2Cu_3O_{6+\delta}$ and $YBa_2Cu_3O_{6+\delta}$ superconductors used in this experiment were affected only slightly by the electron irradiations. Although the Lockheed team used superconductor samples from an earlier batch (note differences between pre-irradiated curves in Figure 26), the results of this experiment are consistent with the Lockheed gamma irradiation results. These results differ considerably, though, from the NRL results presumably due to the differences in bulk versus thick film characteristics. With but one exception, these results support the NRL conclusions that these

materials are sufficiently radiation-hardened to be used in existing space applications given the standard shielding afforded any other space system components.

V. CONCLUSIONS AND RECOMMENDATIONS FOR FUTURE WORK

A. CONCLUSIONS

The results of this research on the effects of high energy electron irradiation of $YBa_2Cu_3O_{6+\delta}$ and $GdBa_2Cu_3O_{6+\delta}$ superconductors indicate that these materials, in bulk applications, are sufficiently hardened to electron irradiation that no special additional shielding should be required for protection against electrons in space or in particle accelerator magnet applications. The results do suggest, however, that there are likely to be microscopic effects in the form of individual channel destructions such that the use of these materials in computer micro-chips aboard satellites or other space-based systems may require special shielding. The experiment also provided insight into possible material incompatability problems with regard to differing thermal expansion rates along the interfaces of contacts on the superconductor.

With the exception of one case ($YBa_2Cu_3O_{6+\delta}$ after 3 Mrad exposure), there were no observable irradiation effects on the superconductivity of thesamples tested. Due to difficulties with the electrical contacts during the measurements, trend analysis was hampered considerably. Nonetheless, the $YBa_2Cu_3O_{6+\delta}$ sample exhibited effects quite similar to the gamma irradiation effects reported by the Lockheed team [Ref. 2]. These effects included a slight broadening of the transition region and a decrease in normal state resistance with increasing irradiations. This decrease in normal state resistance is

somewhat counter-intuitive, but the recurrence in this experiment shows that the effect is not isolated to just one batch of materials.

The $GdBa_2Cu_3O_{6+\delta}$ sample showed no noticeable irradiation effects at all. It was also relatively free of electrical contact difficulties which plagued the $YBa_2Cu_3O_{6+\delta}$ sample throughout the experiment. These reasons form the basis of the conclusion that the $GdBa_2Cu_3O_{6+\delta}$ is a sturdier and more radiation-hardened material than the $YBa_2Cu_3O_{6+\delta}$.

The incidence of sub-77 K superconductivity in the $YBa_2Cu_3O_{6+\delta}$ sample (Figure 25) after a 3 Mrad exposure did not recur for the subsequent exposures.

This, in conjunction with the electrical contact difficulties, supports the conclusion that the microscopic channels are susceptible to damage, but their sheer multitudes make a bulk degradation unlikely in these samples. The fact that such a bulk degradation was apparently observed may be accounted for by the following. The pressed indium contacts were observed to be covered with broken and powdered superconducting material after the first irradiation (note that it had also been thermally cycled between 300K and ~70 K three times at that point). These granules might permit current flow to the rest of the sample by the Josephson effect (electron pair tunneling across the grain boundary interface) or, if the interfacial gaps are too large, the granules could insulate the contacts. If the contacts were overwhelmingly isolated from the sample by these powder grains, the multitudes of available channels would be reduced and a possibility

exists (although seemingly low) that the only available channels would be those damaged by the previous irradiation. If for the next irradiations, the contacts were pressed just slightly to remake a good connection, the number of available channels would increase and the chances of locating an undamaged channel would increase. This could thus prevent any recurrence of the drop in T_c seen in any earlier measurements.

The difficulty with maintaining good electrical contacts with the samples (primarily the $YBa_2Cu_3O_{6+\delta}$ sample) was, as previously described, due to crumbling of the superconductor in the vicinity of the pressed indium contacts. Since no one has reported such difficulties in similar experiments and since the samples here were thermally cycled more times than those in either the Lockheed or NRL studies, the mechanism for this very localized damage appears to be due to differing rates of thermal expansion and compression in adjacent materials.

The thermal expansion rate of the indium may be sufficiently different from that of the $YBa_2Cu_3O_{6+\delta}$ material such that it creates stresses on the interfacial surface of the superconductor. After just a few cyclings between room temperature and T_c the stresses were apparently sufficient to fracture small grains off of the sample, thus creating a surface boundary between the grains and the sample. In addition to allowing the indium contacts to pull out under tension of the platinum wires being connected for measurement, these

boundaries were in one case apparently sufficiently wide to prevent Josephson tunneling, thus inhibiting current flow.

If this was indeed the case, then it may prove to be a serious obstacle to applications wherein the superconducting component may need to be thermally cycled more than an absolute minimum of times. Such foreseeable difficulties could arise for systems where maintenance requirements force the cycling to near room temperature or where a system might be manufactured, tested at operating temperatures and then shipped and stored at room temperature. The following cycle down to operating temperature could, if this assessment is valid, render the system inoperable before it is ever put into end use. This would be inconvenient for land-based applications but it could be a crippling financial and logistical hurdle for space-based applications.

In summary, this experiment has indicated that in a decision as to whether to use $GdBa_2Cu_3O_{6+\delta}$ or $YBa_2Cu_3O_{6+\delta}$ in a high radiation (photon or electron) environment, the $GdBa_2Cu_3O_{6+\delta}$ should be the compound chosen. It appears to be both more resistant to crumbling (whether due to moisture orthermal cycling) and harder to radiation than the $YBa_2Cu_3O_{6+\delta}$. More research remains to be done, however, to confirm that there were not more microscopic effects than detected in this experiment.

B. RECOMMENDATIONS FOR FUTURE WORK

While nearly all indications from this and the other cited experiments show that the materials examined should perform adequately in high radiation environments, more research could confirm the extent

to which microscopic effects occur. Since annealing may have had an effect on the data from each of these experiments (all had annealing times in excess of several hours from the time of irradiation to the time of measurement) research should be done where measurements and irradiations are performed simulataneously at the critical temperature regions. This would have the multiple benefit of minimizing handling and large thermal cyclings of the material, and it could easily be adapted to a small computer-controlled data taking system. This would facilitate data analysis and comparisons with previous data. It would also show the effects of irradiation under operating conditions and may show effects not as yet seen.

In detecting microscopic damage to individual superconducting channels, the four-probe method is somewhat of a hit-or-miss approach. If the contacts had not been so deteriorated, the loss of high temperature (above 77 K) superconductivity observed in this experiment might not have been detected. To better quantify the extent of microscopic damage to channels, perhaps a more useful study would be to examine the magnetic susceptibility of the samples after each irradiation by exploiting the Meissner effect. As the amount of damaged channels increased, the susceptibility would also increase. A complete set of data for several samples and irradiation levels might provide a good data base for empirically-derived damage quantifiers.

Finally, the concern over the thermal expansion rates should be investigated. Superconducting microchips will have to be placed on some sort of substrate which, if it expands too quickly (or slowly)

relative to the superconductor, will fracture the superconducting channels and render the component useless. The same applies for nearly every application of superconductors in that they will undoubtedly share an interface with some different material. These effects may not have been a problem in the past due to the fact that a majority of the conventional superconductors were metals and alloys which were not as prone to crumbling as the newer ceramic compounds. Whether or not this was the mechanism for the damage in this experiment has yet to be confirmed. Even if it was not, the concern should be further investigated due to the strong possibility that it may be a factor elsewhere.

LIST OF REFERENCES

1. Maisch, W. G., et al., "Radiation Effects in High-T_c Superconductors for Space Applications," paper to be published in December 1987 IEEE Transactions on Nuclear Science, 1987.

2. Wolf, S. A., and Krezin, V. Z., eds., Proceedings of the International Workshop on Novel Methods of Superconductivity, Plenum Press, pp. 961-967, 1987.

3. Nisenoff, M., et al., "Naval Applications of Superconductivity," Naval Research News, 37, 1, 1985.

4. Friedman, R. S., et al., Advanced Technology Warfare, Crown Publishers, Inc.,1985.

5. Williams, J. E. C., Superconductivity and its Applications, Pion Ltd., 1970.

6. Chemical Rubber Company, Handbook of Chemistry and Physics, 1986.

7. Chu, C. W., et al., Phys. Rev. Letters 58, 908 (1987).

8. Bednorz, J. G., and Mueller, K. A., Z. Physics B 64, 189 (1986).

9. Kolata, G., "Yb or Not Yb? That Is the Question," Science, Vol. 236, 663, 1987.

10. Eisberg, R. M., and Resnick, R., Quantum Physics of Atoms, Molecules , Solids, Nuclei and Particles, 2nd ed., John Wiley and Sons, Inc., 1985.

11. Kittel, C., Introduction to Solid State Physics, 2nd ed., John Wiley and Sons, Inc., 1956.

12. Lynton, E. A., Superconductivity, 2nd ed, John Wiley and Sons, 1964.

13. Blatt, J. M., Theory of Superconductivity, Academic Press, 1964.

14. Pines, D., The Many-Body Problem—A Lecture Note Reprint Volume, W.A. Benjamin, Inc., p.1175, 1961.

15. Ohanian, H. C., Physics, W.W. Norton and Co., 1985.

16. Kittel, C., and Kroemer, H., Thermal Physics, 2nd ed., W. H. Freeman and Co., 1980.

17. Khurana, A., "High T_c May Not Need Phonons; Supercurrents Increase," Physics Today, 17 (1987).

18. Khurana, A., "Even Lanthanum Copper Oxide Is Superconducting," Physics Today, 17 (1987).

19. Khurana, A., "Superconductivity Seen Above the Boiling Point of Nitrogen," Physics Today, 17 (1987).

20. Chakraverty, B. K., J. Phys. Lett. 40, L99 (1979)

21. Chakraverty, B. K., J. Phys. 42, 1351 (1981).

22. Kittel, C., Introduction to Solid State Physics, 3rd ed., John Wiley and Sons, Inc., 1966.

23. Cava, R. J., et al., Phys. Rev. Lett., 58, 408 (1987).

24. Chu, C. W., et al., Phys. Rev. Lett., 58, 405 (1987).

25. Robinson, A. L., "An Oxygen Key to the New Superconductors," Science, Vol. 263, p. 1064, 1987.

26. Robinson, A. L., "More Superconductivity Questions Than Answers," Science, Vol. 237, p. 248 (1987).

27. Kinchin, G. H., and Pease, R. S., Rept. Prog. Phys., 18, 1, 1

28. Knoll, G. F., Radiation Detection and Measurement, John Wiley and Sons, Inc., 1979.

29. Segré, E., Nuclei and Particles: An Introduction to Nuclear and Subnuclear Physics, W. A. Benjamin, Inc., 1964.

30. Aguilar-Benitez, M., et al., Particle Properties Data Book, Particle Data Group (Lawrence Berkeley Laboratories and CERN), 1986.

31. Berard, R. W., Traverso, T. J., Neutron Form Factors from Elastic Electron-Deuteron Scattering Ratio Experiments at Very Low Momentum Transfers, Master's Thesis, Naval Postgraduate School, Monterey, California, June 1973.

INITIAL DISTRIBUTION LIST

		No. Copies
1.	Defense Technical Information Center Cameron Station Alexandria, VA 22304-6145	2
2.	Library, Code 0142 Naval Postgraduate School Monterey, CA 93943-5002	2
3.	Professor F. R. Buskirk, Code 61Bs Department of Physics Naval Postgraduate School Monterey, CA 93943-5002	3
4.	Professor X. K. Maruyama, Code 61Mp Department of Physics Naval Postgraduate School Monterey, CA 93943-5002	3
5.	L. J. Dries, Code 9740/202 Research and Development Division Lockheed Missiles and Space Company, Inc. 3251 Hanover Street Palo Alto, CA 94304-1191	3
6.	J. C. Ritter, Code 6611 Naval Research Laboratory Washington, D.C. 20375	2
7.	Lt. E. L. Sweigard 6572 Pennacook Court Columbia, MD 21045	3
8.	Lt. J. E. Joynson Department Head School Class 102 Surface Warfare Officers School Command Newport, RI 02841-5012	1

9. Don Snyder, Code 61Ds — 1
Department of Physics
Naval Postgraduate School
Monterey, CA 93943-5000

10. Dr. Elliot H. Weinberg, Director, Code 61 — 1
Navy Center for International Science and Technology
Naval Postgraduate School
Monterey, CA 93943

Thesis
S93522 Sweigard
c.1 Effects of 67.5 MeV electron irradation on Y-Ba-Cu-O and Gd-Ba-Cu-O high-temperature super-conductors.

Thesis
S93522 Sweigard
c.1 Effects of 67.5 MeV electron irradation on Y-Ba-Cu-O and Gd-Ba-Cu-O high-temperature super-conductors.

AMERICAN BINDERY
TOPEKA KANSAS

thesS93522
Effects of 67.5 MeV electron irradation
3 2768 000 77730 4
DUDLEY KNOX LIBRARY